AD-A118 587 HOUSTON UNIV TX DEPT OF ELECTRICAL ENGINEERING F/G 14/2
ELECTROMAGNETIC METHODS OF NONDESTRUCTIVE EVALUATION.(U)
MAY 81 S A LONG, A B EL-KAREH AFOSR-77-3457

UNCLASSIFIED AFOSR-TR-82-0674 NL

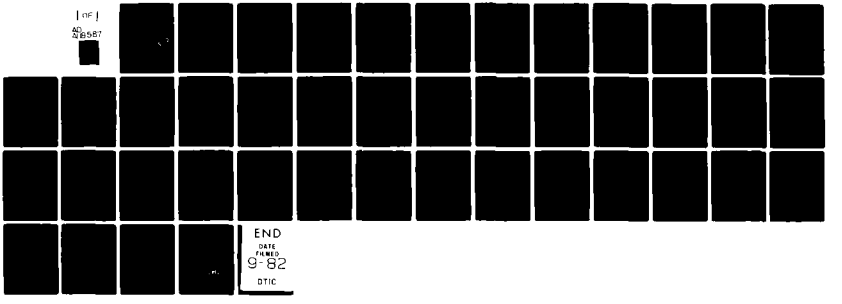

END
DATE FILMED
9-82
DTIC

AFOSR-TR- 82-0674

(15)

ELECTROMAGNETIC METHODS OF NONDESTRUCTIVE EVALUATION

Final Report

through April 30, 1981

Sponsored by the

Air Force Office of Scientific Research

under

Grant No. AFOSR 77-3457

Prepared by

Stuart A. Long
A. B. El-Kareh

Department of Electrical Engineering
University of Houston
Houston, Texas 77004

May 18, 1981

SECURITY CLASSIFICATION OF THIS PAGE (When Data Entered)

REPORT DOCUMENTATION PAGE		READ INSTRUCTIONS BEFORE COMPLETING FORM
1. REPORT NUMBER AFOSR-TR- 82-0674	2. GOVT ACCESSION NO. AD-A118587	3. RECIPIENT'S CATALOG NUMBER
4. TITLE (and Subtitle) ELECTROMAGNETIC METHODS OF NONDESTRUCTIVE EVALUATION		5. TYPE OF REPORT & PERIOD COVERED FINAL 30 Sep 77 - 30 Apr 81
		6. PERFORMING ORG. REPORT NUMBER
7. AUTHOR(s) STUART A LONG A B EL-KAREH		8. CONTRACT OR GRANT NUMBER(s) AFOSR-77-3457
9. PERFORMING ORGANIZATION NAME AND ADDRESS UNIVERSITY OF HOUSTON DEPARTMENT OF ELECTRICAL ENGINEERING HOUSTON, TX 77004		10. PROGRAM ELEMENT, PROJECT, TASK AREA & WORK UNIT NUMBERS 61102F 2307/B2
11. CONTROLLING OFFICE NAME AND ADDRESS AIR FORCE OFFICE OF SCIENTIFIC RESEARCH/NA BOLLING AFB, DC 20332		12. REPORT DATE May 18, 1981
		13. NUMBER OF PAGES 43
14. MONITORING AGENCY NAME & ADDRESS(if different from Controlling Office)		15. SECURITY CLASS. (of this report) UNCLASSIFIED
		15a. DECLASSIFICATION/DOWNGRADING SCHEDULE

16. DISTRIBUTION STATEMENT (of this Report)

Approved for Public Release; Distribution Unlimited.

17. DISTRIBUTION STATEMENT (of the abstract entered in Block 20, if different from Report)

18. SUPPLEMENTARY NOTES

19. KEY WORDS (Continue on reverse side if necessary and identify by block number)
NONDESTRUCTIVE EVALUATION
EDDY CURRENT TESTING
SURFACE ELECTROMAGNETIC WAVES

20. ABSTRACT (Continue on reverse side if necessary and identify by block number)
A study of quantitative nondestructive eddy current testing techniques on nonferromagnetic structural metals has been completed. In addition an investigation was made of electromagnetic surface wave propagation in a dielectric layer on a conducting substrate.

DD FORM 1 JAN 73 1473 EDITION OF 1 NOV 65 IS OBSOLETE 002 UNCLASSIFIED
SECURITY CLASSIFICATION OF THIS PAGE (When Data Entered)

TABLE OF CONTENTS

I. Introduction

The general objective of this program was to further the development of nondestructive evaluation, particularly in relation to its use as a means of quantitatively characterizing performance related properties of structural materials. The principal two areas of emphasis have been low frequency eddy current testing methods for nonferromagnetic metals and microwave testing of dielectric layers on conducting substrates using surface electromagnetic waves.

II. Summary of Progress

A. Eddy Current Testing

The excitation of eddy currents in materials to detect flaws is well developed in practice. The theoretical solutions, however, of even the most basic geometries, which even remotely resemble practical testing situations, have not been attempted until recently. The numerical solutions of Dodd and Deeds [Journal of Applied Physics, Vol. 30, pp. 2823-2838, 1968] and the analytical work by Zaman, Gardner and Long for both cylindrical [IEEE Transactions on Instrumentation and Measurements, March 1981] and planar [Journal of Nondestructive Evaluation, 1981] geometries are the first real attempts to attack the basic eddy current problem on a theoretical level. The results of these studies have application in many practical cases where eddy current methods have been used for years.

The case of a single-turn loop surrounding an imperfectly conducting cylinder has been solved for a slightly restrictive set of physical parameters. The change in complex impedance of the coil was calculated as a function of the geometry of the problem (radii of the coil and core) and of the material properties of the core (conductivity). (See Appendix A)

In a similar fashion the impedance of a loop parallel to and near an infinitely large planar conductor was calculated. This change in complex impedance was found as a function of the size of the coil, the lift-off distance and the conductivity of the material. Again these results bear direct application for practical testing situations employing planar geometries. (See Appendix B)

The results of these previous investigations may also be used to calculate the change in impedance due to a flaw in the conducting material.

A first approximation using only the fields in the unflawed sample has been developed for the usual case of a single coil eddy current system in the presence of a conducting half space. (See Appendix D)

B. Microwave Testing

The investigation of the use of surface electromagnetic waves to measure the thickness and dielectric constant of a dielectric layer supported by a planar conductive substrate has been completed. The theoretical results show that the thickness and the dielectric constant can be measured independently by exciting a surface electromagnetic wave along the layer and the subsequent measurements of its propagation characteristics. The results of this theory have been tested by an experimental investigation of surface waves traveling along 1-2 cm thicknesses of layers of dielectric materials at a frequency of 10 GHz. The resulting predictions of thickness and dielectric constant are found to be quite accurate when applied to samples of known physical properties. The measurement of thinner layers may be accomplished by simply increasing the frequency of operation.

Some addition complexity of the actual experimental apparatus will result, but the same theory will still be valid. Technical details of both the theoretical work and the experimental set-up including a comparison of theory and experiment is included as Appendix C. A more detailed paper is presently under preparation and will be submitted to a suitable journal for publication.

III. Publications and Presentations

Refereed Journals

A. J. M. Zaman, S. A. Long, and C. G. Gardner, "Impedance of a Loop Surrounding a Conducting Cylinder," IEEE Trans. Instrumentations and Measurement, Vol. IM-30, pp. 41-45, March 1981.

A. J. M. Zaman, S. A. Long, and C. G. Gardner, "The Impedance of a Single-Turn Coil Near a Conducting Half-Space," Journal of Nondestructive Evaluation, Vol. 1, No. 3, pp. 183-189, Sept. 1980.

Papers at Technical Meetings

S. A. Long, C. G. Gardner, A. J. M. Zaman, and S. Toomsawasdi, "Impedance of a Circular Coil with a Conductive Cylindrical Core," paper presented at the 12th Symposium on Nondestructive Evaluation Southwest Research Institute, San Antonio, Texas, April 1979.

C. G. Gardner, S. A. Long, and W. Ou, "Nondestructive Evaluation of Dielectric Layers on Conductive Substrates by Microwave Surface Electromagnetic Waves," paper presented at the 12th Symposium on Nondestructive Evaluation, Southwest Research Institute, San Antonio, Texas, April 1979.

S. A. Long, C. G. Gardner, and A. J. M. Zaman, "Impedance of a Loop with a Cylindrical Conducting Core," paper presented at the ARPS/AF Review of Progress in Quantitative NDE, Scripps Institution of Oceanography, LaJolla, California, July 1979.

A. J. M. Zaman, S. A. Long, and C. G. Gardner, "Impedance of a Loop Near a Conducting Half Space," paper presented at the DARPA/AF Review of Progress in Quantitative NDE, Scripps Institution of Oceanography, LaJolla, California, July 1980.

A. J. M. Zaman, C. G. Gardner, and S. A. Long, "The Change in Impedance of a Single-Turn Coil Due to a Void in a Conducting Half Space," paper presented at the 13th Symposium on Nondestructive Evaluation, Southwest Research Institute, San Antonio, Texas, April 1981.

IV. Scientific Personnel

Dr. Stuart A. Long, Principal Investigator

Dr. A. B. El-Kareh, Professor

Dr. C. G. Gardner, Research Professor

Afroz J. M. Zaman, Graduate Student, will receive Ph.D. in Electrical Engineering, August 1981)

Weiming Ou, Graduate Student
(received Master of Science in Electrical Engineering, Sept. 1979)

M. W. McAllister, Graduate Student

S. Toomsawasdi, Graduate Student

APPENDIX A

Impedance of a Loop Surrounding a Conducting Cylinder

IEEE TRANSACTIONS ON INSTRUMENTATION AND MEASUREMENT, VOL. IM-30, NO. 1, MARCH 1981

Impedance of a Loop Surrounding a Conducting Cylinder

AFROZ J. M. ZAMAN, STUART A. LONG, MEMBER, IEEE, AND C. GERALD GARDNER

***Abstract*—The change in complex impedance between an ideal one-turn coil surrounding and coaxial with an infinitely long circular cylinder of conductivity σ and permeability μ and a similar coil without the core has been calculated. From the exact expression, a power series in the quantity δ/b (δ = skin depth; b = radius of core) has been developed. From this result, the change in impedance of a physically realistic multiturn coil can be estimated. The theory permits a rational approach to optimization of the design of eddy-current test coils and provides a possible means of detecting changes in the radius and conductivity of the cylinder.**

I. Introduction

A NOTABLE OMISSION to the present body of knowledge dealing with eddy-current testing is an adequate theoretical basis for the interpretation of changes in the impedance of the test coil. This deficiency remains, even though the fundamental theory is well established, owing to the mathematical difficulties involved in solving the equations for practical test-coil and specimen configurations. A complete solution in analytical form seems to exist for only a few idealized cases which do not necessarily approximate practical problems of current interest.

The problem selected for study in this investigation is that of an idealized one-turn coil (or loop) around and coaxial with a long, solid, electrically conducting cylinder. This arrangement is illustrated in Fig. 1 and shows the loop with radius a and the core with radius b and conductivity σ. The theoretical treatment will assume that the core is infinitely long. (This approximation should produce very small errors as long as the distance from the position of the loop to either end of the core is large compared to the dimensions of the loop itself.) This problem has the advantage of being simple enough to permit a meaningful approximate solution to be found while still corresponding to a practical eddy-current testing situation. The results show how the complex impedance of the test coil changes when a cylindrical specimen is placed inside the loop and how this impedance is a function of the geometrical and material parameters of the cylindrical core.

II. Theory

A theoretical treatment of a geometrically similar problem has been previously reported by Islam [1]. In that work, however, the emphasis was on the radiation properties of the configuration and thus only a high-frequency approximation was attempted for the case of a magnetically permeable cylindrical core. The case of interest in this work, that of an electrically conducting core at much lower frequencies, may be attacked in a similar fashion but is essentially a completely different problem. A previous paper by Dodd and Deeds [2] investigates this configuration but its solutions are left in the form of complicated integrals which must be evaluated numerically. From Maxwell's equations for time-harmonic fields one may derive the wave equation for the magnetic vector potential $\boldsymbol{A}$ in terms of the impressed current density $\boldsymbol{J}$.

$$\nabla^2 \boldsymbol{A} + k^2 \boldsymbol{A} = -\mu \boldsymbol{J}. \tag{1}$$

Using the standard eddy-current approximation of neglecting the displacement current terms and recognizing that the vector potential has only a $\hat{\phi}$ component which depends on r and z, the left-hand side of the equation becomes

$$\nabla^2 \boldsymbol{A} = \hat{\phi}\left(\nabla^2 A_\phi - \frac{A_\phi}{r^2}\right) = \hat{\phi}\left[\frac{1}{r}\frac{\partial}{\partial r}\left(r\frac{\partial A_\phi}{\partial r}\right) + \frac{\partial^2 A_\phi}{\partial z^2} - \frac{A_\phi}{r^2}\right]$$

$$= \hat{\phi}\left[\frac{\partial^2 A_\phi}{\partial r^2} + \frac{1}{r}\frac{\partial A_\phi}{\partial r} - \frac{A_\phi}{r^2} + \frac{\partial^2 A_\phi}{\partial z^2}\right]. \tag{2}$$

Equating this expression to the source terms due to the loop current and the induced eddy currents one obtains the equation for the vector potential in each of the regions shown in Fig. 1.

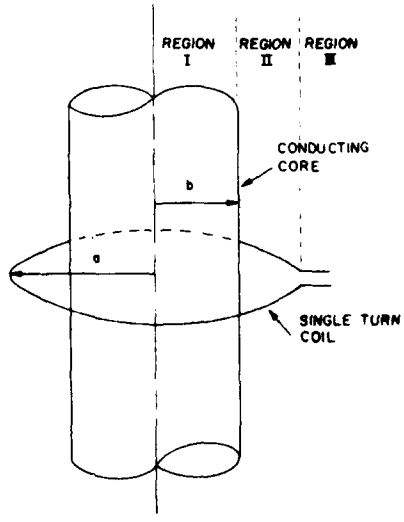

Fig. 1. Loop with a cylindrical core.

Manuscript received October 1, 1979; revised September 9, 1980. This work was supported in part by the U.S. Air Force Office of Scientific Research under Grant 77-3457.

The authors are with the Electrical Engineering Department, University of Houston, Houston, TX 77004.

0018-9456/81/0200-0041$00.75 © 1981 IEEE

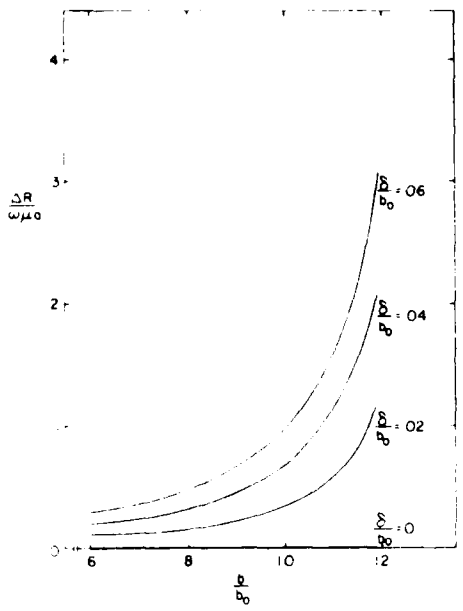

Fig. 2. Normalized resistance versus core radius

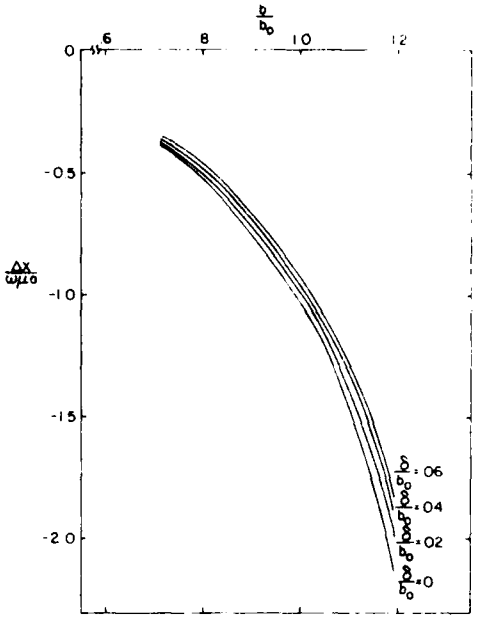

Fig. 3. Normalized reactance versus core radius

$$\frac{\partial^2 A_\phi}{\partial r^2} + \frac{1}{r}\frac{\partial A_\phi}{\partial r} - \frac{A_\phi}{r^2} + \frac{\partial^2 A_\phi}{\partial z^2} = \begin{cases} -\mu_0 i_0 \delta(z)\delta(a-r), & r > b \\ j\omega\mu\sigma A_\phi, & r < b \end{cases} \quad (3)$$

where μ_0 is the permeability of free space, i_0 is the magnitude of the impressed loop current, ω is the angular frequency of the time-harmonic fields, and μ and σ are the permeability and conductivity of the core. The presence of the impressed loop current at $z = 0$, $r = a$ is represented by the two δ functions.

The solution to the equation may be found using a cosine transform.

$$A_\phi(r, z) = \frac{1}{\pi}\int_0^\infty g(r, k)\cos kz\, dk \quad (4)$$

with the following functions defined for each of the three regions:

$$g(r, k) = \begin{cases} C_1 I_1[\sqrt{(k^2 + j\kappa^2)}r], & r < b \\ C_2 I_1(kr) + C_3 K_1(kr), & b < r < a \\ C_4 K_1(kr), & r > a \end{cases} \quad (5)$$

where I_1 and K_1 are the modified Bessel functions of order one, $\kappa^2 = \omega\mu\sigma$, and C_1, C_2, C_3, and C_4 are constants to be determined by the boundary conditions.

Since the quantity of primary interest is the vector potential in the vicinity of the loop, the simplest expression is that for Region III for which only C_4 needs to be found from the standard boundary conditions.

$$C_4 = \mu_0 i_0 a\left\{I_1(ka) + \left[\frac{kbI_0(kb)I_1(\gamma) - \gamma I_0(\gamma)I_1(kb)}{kbI_1(\gamma)K_0(kb) + \gamma I_0(\gamma)K_1(kb)}\right]K_1(ka)\right\} \quad (6)$$

where I_0 and K_0 are the modified Bessel functions of order zero and $\gamma = \sqrt{(kb)^2 + j(\kappa b)^2}$. Using this expression the value of A_ϕ along the loop at $z = 0$, $r = a$ can be found.

$$A_\phi(a, 0) = \frac{\mu_0 i_0 a}{\pi}\int_0^\infty I_1(ka)K_1(ka)\, dk + \frac{\mu_0 i_0 a}{\pi} \cdot \int_0^\infty \left[\frac{kbI_0(kb)I_1(\gamma) - \gamma I_0(\gamma)I_1(kb)}{kbI_1(\gamma)K_0(kb) + \gamma I_0(\gamma)K_1(kb)}\right]K_1^2(ka)\, dk \quad (7)$$

The first of these integrals can be shown to be exactly the contribution to the vector potential due to the loop itself if the core were not present at all. (This term is singular in nature.) The second integral is the contribution due to the eddy currents and thus represents the difference in the vector potential with and without the core present. This term now called ΔA_ϕ may be expanded as an asymptotic series.

$$\Delta A_\phi = \frac{\mu_0 i_0 a}{\pi}\left[-\int_0^\infty \frac{I_1(kb)K_1^2(ka)}{K_1(kb)}\, dk + \int_0^\infty \frac{I(\gamma)K_1^2(ka)}{K_1^2(kb)}\, dk - \int_0^\infty \frac{I^2(\gamma)kbK_0(kb)K_1^2(ka)}{K_1^3(kb)}\, dk + \int_0^\infty \frac{I^3(\gamma)(kb)^2K_0^2(kb)K_1^2(ka)}{K_1^4(kb)}\, dk + \cdots\right] \quad (8)$$

where

$$T(\gamma) = \frac{1}{\gamma}\frac{I_1(\gamma)}{I_0(\gamma)}.$$

It should be noted that the dependence of ΔA_ϕ on the material parameters μ and σ of the core is completely contained in the $I(\gamma)$ term. For certain cases of practical interest, κ is large compared to values of k within the range for which the integrands in (8) are appreciable. For such cases, γ (and hence $I(\gamma)$), is nearly independent of k. Indeed, as κ becomes sufficiently large (corresponding to a core conductivity approaching infinity) we have

$$\gamma \to \sqrt{j\kappa h} = (1+j)(h/\delta)$$

where $\delta = \sqrt{2/\omega\mu\sigma}$, the skin depth. We, therefore, expect that for small but nonvanishing skin depth, $T(\gamma)$ may be adequately represented by an asymptotic series in (δ/b). Using the standard asymptotic series for the modified Bessel functions we find

$$I(\gamma) \to \frac{1}{\gamma} - \frac{1}{2\gamma^2} - \frac{1}{8\gamma^3} + \cdots. \tag{9}$$

Expanding γ^{-1} as a power series in k/κ, and neglecting terms of order higher than $(\delta/b)^3$, we find

$$I(\gamma) \to \frac{(1-j)}{2}\left(\frac{\delta}{b}\right) + \frac{j}{4}\left(\frac{\delta}{b}\right)^2 + \frac{(1+j)}{8}\left(\frac{\delta}{b}\right)^3\left[(kb)^2 + \frac{1}{4}\right]. \tag{10}$$

Note that the lowest order term affected by the k dependence of γ is the $(\delta/b)^3$ term. For the range of geometrical and material parameters considered in subsequent numerical work, the cubic term contributes negligibly to the final result.

One may then separate the contributions to ΔA_ϕ into real and imaginary parts

$$\begin{aligned}\Delta A_\phi = {} & \frac{\mu_0 a_0}{\pi}\left(\frac{a}{b}\right)\left\{-N_0\left(\frac{a}{b}\right) + \frac{1}{2}\left(\frac{\delta}{b}\right)N_1\left(\frac{a}{b}\right)\right. \\ & - \frac{1}{4}\left(\frac{\delta}{b}\right)^2\left[-\frac{1}{8}N_1\left(\frac{a}{b}\right) + N_2\left(\frac{a}{b}\right)\right. \\ & \left.\left. - \frac{1}{2}N_3\left(\frac{a}{b}\right) + N_4\left(\frac{a}{b}\right)\right]\right\} \\ & - j\frac{\mu_0 a_0}{\pi}\left(\frac{a}{b}\right)\left\{\frac{1}{2}\left(\frac{\delta}{b}\right)N_1\left(\frac{a}{b}\right) - \frac{1}{2}\left(\frac{\delta}{b}\right)^2\left[\frac{1}{2}N_1\left(\frac{a}{b}\right)\right.\right. \\ & \left. + N_2\left(\frac{a}{b}\right)\right] + \frac{1}{4}\left(\frac{\delta}{b}\right)^3\left[-\frac{1}{8}N_1\left(\frac{a}{b}\right) + N_2\left(\frac{a}{b}\right) - \frac{1}{2}N_3\left(\frac{a}{b}\right)\right. \\ & \left.\left. + N_4\left(\frac{a}{b}\right)\right]\right\}\end{aligned} \tag{11}$$

where the following integrals have been defined and are seen to be only a function of the ratio a/b ($\eta = kb$)

$$N_0\left(\frac{a}{b}\right) = \int_0^\infty \frac{I_1(\eta)K_1^2\left(\eta\frac{a}{b}\right)}{K_1(\eta)}\,d\eta \tag{12}$$

$$N_1\left(\frac{a}{b}\right) = \int_0^\infty \frac{K_1^2\left(\eta\frac{a}{b}\right)}{K_1^2(\eta)}\,d\eta \tag{13}$$

$$N_2\left(\frac{a}{b}\right) = \int_0^\infty \frac{\eta K_0(\eta)K_1^2\left(\eta\frac{a}{b}\right)}{K_1^3(\eta)}\,d\eta \tag{14}$$

$$N_3\left(\frac{a}{b}\right) = \int_0^\infty \frac{\eta^2 K_1^2\left(\eta\frac{a}{b}\right)d\eta}{K_1^3(\eta)} \tag{15}$$

$$N_4\left(\frac{a}{b}\right) = \int_0^\infty \frac{\eta^2 K_0^2(\eta)K_1^2\left(\eta\frac{a}{b}\right)}{K_1^4(\eta)}\,d\eta. \tag{16}$$

The apparent change in the driving point impedance of the loop is

$$\Delta Z = \Delta R + j\omega\Delta L = \frac{j\omega\Delta A_\phi 2\pi a}{i_0} \tag{17}$$

From the previous expressions, the changes in inductance and resistance can be found to third order in δ/b

$$\begin{aligned}\Delta L = {} & -2\mu_0\frac{a^2}{b}\left\{N_0\left(\frac{a}{b}\right) - \frac{1}{2}\left(\frac{\delta}{b}\right)N_1\left(\frac{a}{b}\right)\right. \\ & + \frac{1}{4}\left(\frac{\delta}{b}\right)^3\left[-\frac{1}{8}N_1\left(\frac{a}{b}\right) + N_2\left(\frac{a}{b}\right)\right. \\ & \left.\left. - \frac{1}{2}N_3\left(\frac{a}{b}\right) + N_4\left(\frac{a}{b}\right)\right]\right\}\end{aligned} \tag{18}$$

$$\begin{aligned}\Delta R = {} & 2\omega\mu_0\frac{a^2}{b}\left\{\frac{1}{2}\left(\frac{\delta}{b}\right)N_1\left(\frac{a}{b}\right) - \frac{1}{2}\left(\frac{\delta}{b}\right)^2\left[\frac{1}{2}N_1\left(\frac{a}{b}\right) + N_2\left(\frac{a}{b}\right)\right]\right. \\ & + \frac{1}{4}\left(\frac{\delta}{b}\right)^3\left[-\frac{1}{8}N_1\left(\frac{a}{b}\right) + N_2\left(\frac{a}{b}\right)\right. \\ & \left.\left. - \frac{1}{2}N_3\left(\frac{a}{b}\right) + N_4\left(\frac{a}{b}\right)\right]\right\}.\end{aligned} \tag{19}$$

To obtain numerical values for ΔL and ΔR it is first necessary to evaluate the integrals N_0, N_1, N_2, N_3, and N_4. Although they cannot be evaluated analytically they can be found numerically for fixed values of the geometrical parameter a/b. Once these integrals are evaluated, the expressions are each seen to be a power series in the parameter δ/b which contains the electrical properties of the core material. One should note that for the case of a perfectly conducting core (i.e., $\delta/b = 0$)

$$\Delta L = \frac{-2\mu_0 a^2}{b}N_0\left(\frac{a}{b}\right)$$

and $\Delta R = 0$. This is a reasonable result which shows a decrease in the inductance but no change in the resistance since no losses are possible. The effect of a large but finite conductivity is seen to diminish the amount of decrease found for the perfectly conducting case and to add a finite, positive apparent resistance.

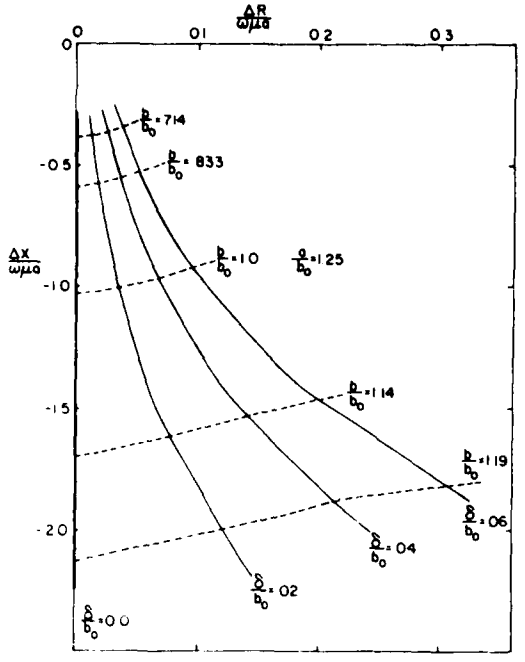

Fig. 4. Resistance versus reactance as core radius changes.

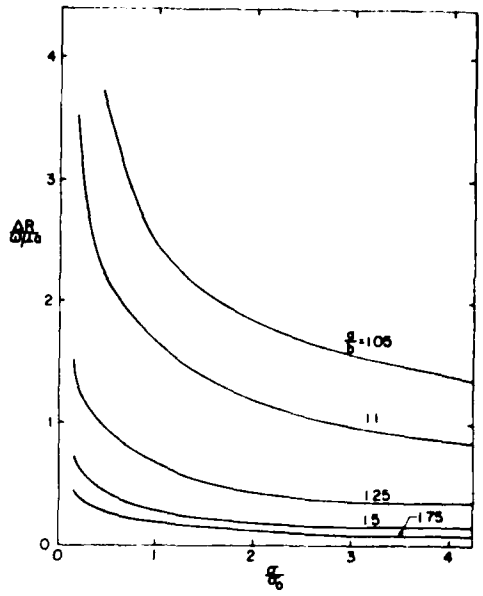

Fig. 5. Normalized resistance versus conductivity.

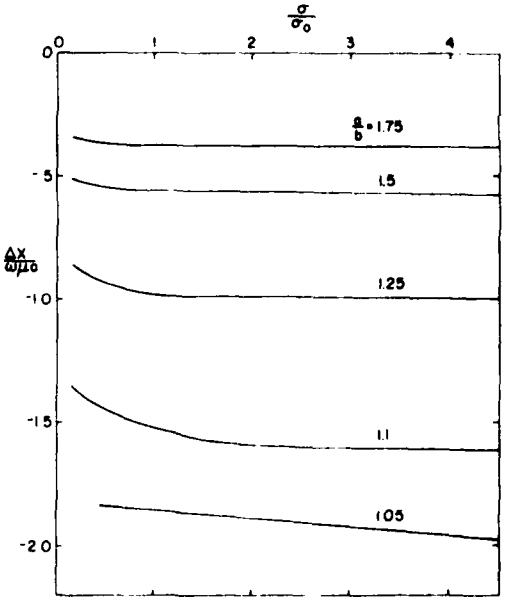

Fig. 6. Normalized reactance versus conductivity.

III. Results

To facilitate the evaluation of ΔL and ΔR for practical cases the integrals N_0, N_1, N_2, N_3, and N_4 were evaluated for several values of a/b varying from a value of 1.05 to 2.0. Using these results, the values of ΔR and ΔL can be calculated through terms of order $(\delta/b)^3$. Accuracy of the results depends critically on the assumption that δ/b remains small with respect to one.

For the case of an aluminum core with a $\frac{3}{4}$-in diameter we find $\delta = 0.0826\sqrt{f}$ which for $f = 50$ kHz yields a skin depth $\delta = 0.37$ mm resulting in a value of $\delta/b = 0.0388$. Thus for this practical case we are well within the assumptions used in the derivations.

To generalize the results somewhat, the normalized quantities $\Delta R/\omega\mu a$ and $\Delta X/\omega\mu a$ have been plotted in the remaining figures ($\Delta X = \omega\Delta L$). It should be noted that each of these quantities is unitless. The most obvious graphical presentations would be those of ΔR and ΔL versus the geometrical parameter a/b and the material parameter δ/b. Unfortunately, this direct approach does not correspond to the usual parameters which may be subject to change. Assuming that the practical testing situation consists of a cylindrical sample moving through a fixed coil, the quantities which may change are actually the radius of the core b and the conductivity of the core material σ. To illustrate the changes in impedance for variations in b about a nominal radius b_0, the graphs in Figs. 2 and 3 are shown. In Fig. 2, the normalized change in resistance is shown versus the quantity b/b_0. The nominal radius b_0 may be any value as long as our restriction of $\delta/b_0 \ll 1$ is satisfied. The value of $a/b_0 = 1.25$ was chosen to be representative of a real coil design which couples strongly with the core. A family of curves is also shown for several values of δ/b_0.

It is noted that all the curves approach zero as b/b_0 is decreased and become very large as b/b_0 approaches 1.25 which is the position of the driving loop. A similar set of curves is shown in Fig. 3 for the change in reactance. Again as expected, the change in reactance approaches zero as the core radius decreases and becomes a very large negative value for b/b_0 near 1.25. It should be noted that changes in the parameter δ/b_0 have a relatively small effect on ΔX as compared to their effect on ΔR. The same functional dependence is also illustrated in Fig. 4. The solid curves show the normalized resistance plotted versus the normalized reactance as b/b_0 is varied. Changes in

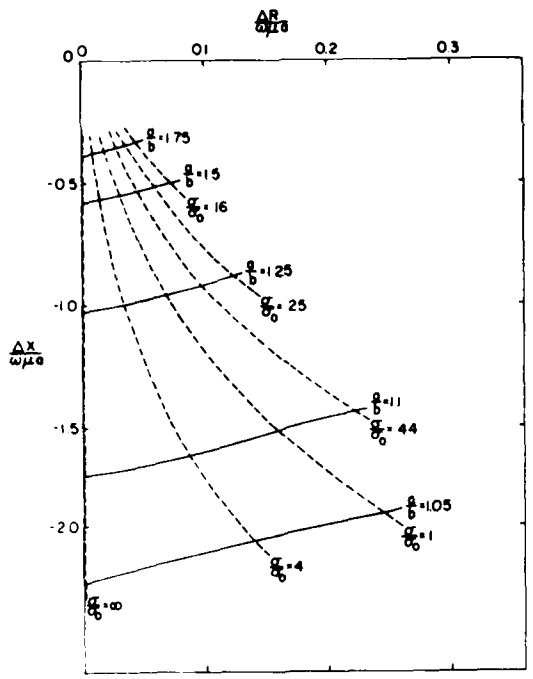

Fig. 7. Resistance versus reactance as conductivity changes.

the complex impedance can be seen for varying radii for each of four values of δ/b_0.

The effect of changes in conductivity of the core on the resistance and the reactance are shown in Figs. 5 and 6. The conductivity is again normalized with respect to a σ_0 near that of aluminum. (However, σ_0 is actually arbitrary as long as the condition that $\delta/b \ll 1$ is still satisfied.) The limiting behavior is again logical showing the resistance approaching zero for large conductivities and zero for very small values. The reactance is seen to approach the "perfect conductor" case as σ increases. The region where σ becomes small violates the assumption on δ/b and, therefore, the behavior of these curves has no meaning in this region. The resistance versus the reactance is shown in the solid lines of Fig. 7. As the conductivity decreases from the perfect conductor case, ΔR is seen to increase while ΔX becomes less negative. Each of these curves terminates in the region where the assumption that $\delta/b \ll 1$ begins to break down.

With the aid of Figs. 4 and 7 one may ascertain the behavior of changes in both the resistance and reactance for any percent change in either the radius of the core of its conductivity. The functional change in impedance is quite different for the two parameters. This characteristic may, therefore, be utilized in practical testing to determine changes in sample radius and conductivity of rods and tubes with wall thickness greater than several skin depths.

REFERENCES

[1] A. M. Islam, "A theoretical treatment of low-frequency loop antennas with permeable cores," *IEEE Trans. Antennas Propagat.*, vol. AP-11, no. 2, pp. 162-169, Mar. 1963.

[2] C. V. Dodd and W. E. Deeds, "Analytical solutions to eddy-current probe-coil problems," *J. Appl. Phys.*, vol. 39, no. 6, pp. 2829-2838, May 1968.

APPENDIX B

The Impedance of a Single-Turn Coil a Conducting Half Space

Journal of Nondestructive Evaluation, Vol. 1, No. 3, 1980

The Impedance of a Single-Turn Coil Near a Conducting Half Space

Afroz J. M. Zaman,[1] Stuart A. Long,[1] and C. Gerald Gardner[1]

Received June 4, 1980

The change in complex impedance between an ideal one-turn circular coil located above and parallel to a conducting half space with respect to a similar isolated coil has been calculated. From this result, a series expansion of the integrand allows the solution to be approximated by terms expressed as complete elliptic integrals. Results have been calculated for the change in impedance as a function of the liftoff distance and the conductivity of the half space for a coil of representative radius.

KEY WORDS: eddy current; impedance; liftoff; conductivity.

1. INTRODUCTION

The eddy current method of nondestructive evaluation entails the induction of eddy currents in a conductive test object by a time-varying field produced by a suitable distribution of impressed currents (via an excitation or primary coil), and the detection of the resultant field, usually by an inductive search coil, which may be either a separate secondary coil or the primary coil itself (see Fig. 1). The method is ordinarily used at frequencies sufficiently low to neglect effects due to displacement current; hence a theoretical analysis entails calculating either a transfer impedance for a primary coil and secondary coil in the presence of the test object, or the calculation of the self-impedance of a primary coil in the presence of the test object. In practice, one often needs only the change in impedance produced by the test object or by changes in the nominal properties of the test object (e.g., changes in its geometry or position with respect to the test coil or coils, or distributed or localized changes in the resistivity of the test object). The most general case, allowing arbitrary configurations of primary and secondary coils and arbitrary test objects, can be handled only by numerical methods. Certain idealized arrangements can be treated analytically either exactly or in useful approximation. In virtually all cases of practical interest, the analysis eventually reduces to the evaluation of certain integrals that cannot be expressed in closed form in terms of standard transcendental functions.

In this paper, we discuss the case of a one-turn circular coil located above and parallel to the surface of a homogeneous conductive half space. From the standard boundary value problem approach, we obtain the general expression for the change in coil impedance, ΔZ, produced by the half space; ΔZ is given in terms of an integral over a separation parameter. A series expansion of one term in the integrand permits the integral to be expressed as a series of terms, each of which is expressible in terms of complete elliptic integrals. The leading terms of this series approximate ΔZ asymptotically for sufficiently small values of skin depth of the half space.

The problem addressed here has previously been treated by Cheng,[1] who evaluated ΔZ by numerical methods for various choices of the relevant parameters. Similarly, Dodd and Deeds[2] have devised a digital computer program capable of handling cir-

[1]Department of Electrical Engineering, University of Houston, Houston, Texas 77004.

0195-9298/80/0900-0183$03.00/0

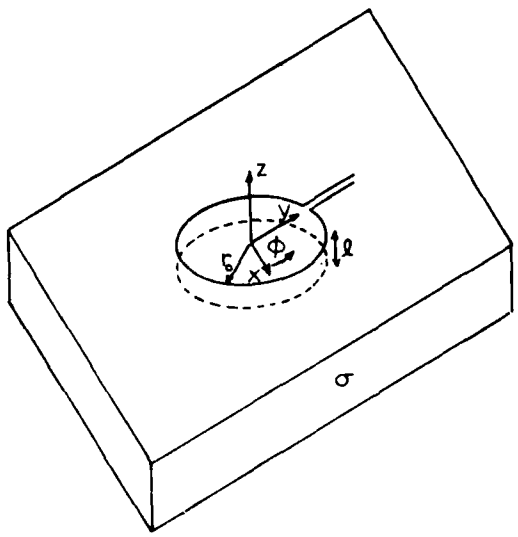

Fig. 1. Geometrical configuration of loop near a conductor.

cular test coils in the presence of layered planar and coaxial cylindrical test objects. Such brute force numerical procedures are valuable for design purposes, but have the disadvantage of somewhat concealing the essentially simple manner in which the final result depends upon the parameters of the problem. The approach taken here, while less universal than the purely numerical approach, results in relatively simple, though approximate and restricted, formulas for ΔZ in terms of the basic parameters of the problem. For illustrative and comparative purposes, some selected numerical examples are also given.

2. THEORETICAL ANALYSIS

The basic geometry of the problem is shown in Fig. 1, and consists of a loop of radius r_0 oriented parallel to and at a distance l above a homogeneous half space of conductivity σ. Beginning with the basic equation for the vector potential,

$$\nabla^2\mathbf{A}+k^2\mathbf{A}=-\mu I(t)\frac{\delta(r_0-r)}{r}\delta(l-z) \qquad (1)$$

and noting the symmetry of the problem, it is seen that the only component of the vector potential present is the circumferential component, A_ϕ, and that A_ϕ is a function of r and z only. Making the usual low-frequency, quasi-static approximation that the $k^2\mathbf{A}$ term is negligible for $z>0$, we have

$$\nabla^2\mathbf{A}=\frac{\partial^2 A_\phi}{\partial r^2}+\frac{1}{r}\frac{\partial A_\phi}{\partial r}+\frac{\partial^2 A_\phi}{\partial z^2}-\frac{A_\phi}{r^2}=0 \quad \text{for } z>0 \qquad (2)$$

and, with $k^2\doteq -j\omega\mu\sigma$ for $z<0$,

$$\frac{\partial^2 A_\phi}{\partial r^2}+\frac{1}{r}\frac{\partial A_\phi}{\partial r}+\frac{\partial^2 A_\phi}{\partial z^2}-\frac{A_\phi}{r^2}-j\omega\mu\sigma A_\phi=0 \quad \text{for } z<0 \qquad (3)$$

Solving by the separation of variables technique yields the following expression for the general solution to Eqs. (2) and (3):

$$A_\phi(r,z)=\int_0^\infty\left[A(\alpha)e^{\alpha z}+B(\alpha)e^{-\alpha z}\right]\times\left[C(\alpha)J_1(\alpha r)+D(\alpha)Y_1(\alpha r)\right]d\alpha \qquad (4)$$

where α is the separation constant. Since z may become infinitely large in the region $z>l$, the coefficient $A(\alpha)$ must equal zero. Similarly, in the region $z<0$, $B(\alpha)$ must also equal zero, and since the origin is included in all regions, then $D(\alpha)$ must equal zero in each:

$$A_{\phi 1}(r,z)=\int_0^\infty B_1 e^{-\alpha z}J_1(\alpha r)\,d\alpha \qquad z>l>0 \qquad (5)$$

$$A_{\phi 2}(r,z)=\int_0^\infty\left[C_2e^{\alpha z}+B_2e^{-\alpha z}\right]J_1(\alpha r)\,d\alpha \qquad l>z>0 \qquad (6)$$

$$A_{\phi 3}(r,z)=\int_0^\infty C_3e^{\alpha_1 z}J_1(\alpha r)\,d\alpha \qquad z<0 \qquad (7)$$

where $\alpha_1^2=\alpha^2+j\omega\mu\sigma$.

Since the electric field is proportional to A_ϕ, the boundary conditions for the tangential electric field can be satisfied by equating the values of A_ϕ at the $z=l$ plane:

$$\int_0^\infty B_1e^{-\alpha l}J_1(\alpha r)\,d\alpha=\int_0^\infty\left(C_2e^{\alpha l}+B_2e^{-\alpha l}\right)J_1(\alpha r)\,d\alpha \qquad (8)$$

Multiplying both sides by the integral operator $\int_0^\infty\{\cdots\}J_1(\alpha' r)r\,dr$ and using the Fourier-Bessel identity,[3]

$$\int_0^\infty J_1(\alpha r)J_1(\alpha' r)r\,dr=\frac{\delta(\alpha-\alpha')}{\alpha} \tag{9}$$

gives the following result:

$$\frac{B_1 e^{-\alpha' l}}{\alpha'}=\frac{C_2}{\alpha'}e^{\alpha' l}+\frac{B_2}{\alpha'}e^{-\alpha' l} \tag{10}$$

or

$$B_1 e^{-\alpha l}=C_2 e^{\alpha l}+B_2 e^{-\alpha l} \tag{11}$$

The radial component of the magnetic field can also be found from the vector potential, $H_r=-(\partial/\partial z)A_\phi$. H_r is discontinuous at the position of the loop ($r=r_0$, $z=l$) by an amount equal to the surface current density there:

$$\left[-\frac{\partial}{\partial z}A_{\phi 1}+\frac{\partial}{\partial z}A_{\phi 2}\right]_{z=l}=\mu I\delta(r-r_0) \tag{12}$$

or

$$-B_1 e^{-\alpha l}=C_2 e^{\alpha l}-B_2 e^{-\alpha l}-\mu I r_0 J_1(\alpha r_0) \tag{13}$$

Similarly, the boundary conditions may also be applied at $z=0$, where both E_ϕ and H_r are continuous, yielding

$$C_2+B_2=C_3 \tag{14}$$

and

$$C_2-B_2=\frac{\alpha_1}{\alpha}C_3 \tag{15}$$

These four equations (11, 13, 14, and 15) can then be solved for the constants B_1, C_2, B_2, and C_3 and used in Eqs. (5), (6), and (7) to evaluate the vector potential.

Since our principle interest lies in evaluating the vector potential at the location of the loop, the most direct route is to evaluate the constant B_1:

$$B_1=\frac{\mu I r_0 J_1(\alpha r_0)}{2}\left[e^{\alpha l}+e^{-\alpha l}\frac{(1-(\alpha_1/\alpha))}{(1+(\alpha_1/\alpha))}\right] \tag{16}$$

Thus

$$A_{\phi 1}(r,z)=\frac{\mu I r_0}{2}\int_0^\infty J_1(\alpha r_0)J_1(\alpha r)e^{(-\alpha z-\alpha l)}\times\left[e^{+2\alpha l}+\left(\frac{\alpha-\alpha_1}{\alpha+\alpha_1}\right)\right]d\alpha \tag{17}$$

The two terms in the square brackets represent, respectively, the vector potential due to the loop itself and that due to the currents induced in the conducting plane. This second term, due to the conductive half space, will produce the change in impedance from the case of the isolated loop to the case of the loop near the plane. This change in vector potential is thus given by this second term:

$$\Delta A_{\phi 1}(r,z)=\frac{\mu I r_0}{2}\int_0^\infty J_1(\alpha r_0)J_1(\alpha r)e^{-\alpha(z+l)}\times\left(\frac{\alpha-\alpha_1}{\alpha+\alpha_1}\right)d\alpha \tag{18}$$

This change in vector potential can be used to calculate the change in impedance due to the presence of the conductor by integrating the tangential electric field around the position of the loop:

$$\Delta Z=\frac{-\oint\Delta\mathbf{E}\cdot d\mathbf{l}}{I}=j\omega\frac{2\pi r_0}{I}\Delta A_{\phi 1}(r_0,l) \tag{19}$$

since $\Delta\mathbf{E}=-j\omega\Delta A_{\phi 1}\hat{\phi}$; then

$$\Delta Z=\pi\omega r_0^2\mu\int_0^\infty J_1^2(\alpha r_0)e^{-2\alpha l}\left(\frac{\alpha-\alpha_1}{\alpha+\alpha_1}\right)d\alpha \tag{20}$$

The integrand factor $(\alpha-\alpha_1)/(\alpha+\alpha_1)$, essentially a reflection factor, has modulus equal to or less than unity, the extreme value being assumed for $\alpha=0$ and $\alpha=\infty$. The integrand factor $J_1^2(\alpha r_0)$ guarantees that the value of the integral is negligibly affected by values of α greater than about $10/r_0$. Practical values of r_0 are usually of the order of 10^{-2}m. For such values of r_0, the importance range for α is $0\leqslant\alpha\leqslant 10^3$ m^{-1}, while the quantity $\omega\mu\sigma$ [$=2/(\text{skin depth})^2$] is, in many practical cases, of the order of 10^7 (e.g., for aluminum at 50 KHz, $\omega\mu\sigma=1.5\times10^7$). For such cases, $\alpha^2/\omega\mu\sigma\leqslant 0.1$, and $(\alpha-\alpha_1)/(\alpha+\alpha_1)$ may be expanded as a power series in $\alpha/\sqrt{\omega\mu\sigma}$:

$$\frac{\alpha-\alpha_1}{\alpha+\alpha_1}=-1+\frac{2}{\sqrt{j}}\frac{\alpha}{\kappa}-\frac{2}{j}\frac{\alpha^2}{\kappa^2}+\cdots$$

$$=-1+(1-j)(\alpha\delta)+j(\alpha\delta)^2+\cdots \tag{21}$$

where $\delta=\sqrt{2/\omega\mu\sigma}$, and $\kappa=\sqrt{\omega\mu\sigma}$.

We expect the series above to converge rapidly provided $\alpha\delta\ll 1$. As we shall presently show, it is convenient to adopt r_0 as a characteristic length.

Since the value of ΔZ is determined almost entirely by values of α for which $\alpha r_0 \leq 10$, we have rapid convergence of the integrated series if $\delta/r_0 \ll 1/10$. Separating ΔZ into real and imaginary parts, we have

$$\Delta Z = \Delta R + j\Delta X \tag{22}$$

$$\Delta X = -\mu\omega\pi r_0^2\left\{\int_0^\infty J_1^2(\alpha r_0)e^{-2\alpha l}\,d\alpha - \int_0^\infty \delta J_1^2(\alpha r_0)e^{-2\alpha l}\alpha\,d\alpha\right\} \tag{23}$$

$$\Delta R = \mu\omega\pi r_0^2\left\{\int_0^\infty \delta J_1^2(\alpha r_0)e^{-2\alpha l}\alpha\,d\alpha - \int_0^\infty \delta^2 J_1^2(\alpha r_0)e^{-2\alpha l}\alpha^2\,d\alpha\right\} \tag{24}$$

These changes in resistance and reactance can be represented by three integrals:

$$\Delta X = -\pi\omega\mu r_0\left(I_1(\beta) - \left(\frac{\delta}{r_0}\right)I_2(\beta)\right) \tag{25}$$

$$\Delta R = \pi\omega\mu r_0\left(\left(\frac{\delta}{r_0}\right)I_2(\beta) - \left(\frac{\delta}{r_0}\right)^2 I_3(\beta)\right) \tag{26}$$

where

$$\beta \doteq 2l/r_0 \tag{27}$$

and

$$I_1(\beta) \doteq \int_0^\infty J_1^2(x)e^{-\beta x}\,dx \tag{28}$$

$$I_2(\beta) \doteq -\frac{d}{d\beta}I_1(\beta) \tag{29}$$

$$I_3(\beta) \doteq \frac{d^2}{d\beta^2}I_1(\beta) \tag{30}$$

$I_1(\beta)$ is just the Laplace transform of $J_1^2(x)$[4]

$$I_1(\beta) = \frac{1}{\pi}Q_{1/2}\left(1+\frac{1}{2}\beta^2\right) \tag{31}$$

where $Q_{1/2}$ is the Legendre function of the second kind of order 1/2.

$I_2(\beta)$ is therefore given by

$$I_2(\beta) = -\frac{\beta}{\pi}Q'_{1/2}\left(1+\frac{1}{2}\beta^2\right) \tag{32}$$

where the prime indicates differentiation with respect to the argument. The required derivative may be found from the recursion relation[5]

$$(x^2-1)Q'_{1/2}(x) = \frac{x}{2}Q_{1/2}(x) - \tfrac{1}{2}Q_{-1/2}(x) \tag{33}$$

For convenience in evaluation, both $Q_{1/2}$ and $Q_{-1/2}$ may be expressed in terms of complete elliptic integrals[5]:

$$Q_{1/2}(x) = x\left(\frac{2}{x+1}\right)^{1/2}K\left[\left(\frac{2}{x+1}\right)^{1/2}\right] - [2(x+1)]^{1/2}E\left[\left(\frac{2}{x+1}\right)^{1/2}\right] \tag{34}$$

$$Q_{-1/2}(x) = \left(\frac{2}{x+1}\right)^{1/2}K\left[\left(\frac{2}{x+1}\right)^{1/2}\right] \tag{35}$$

where $K(k)$ and $E(k)$ are, respectively, the complete elliptic integrals of the first and second kind of modulus k:

$$K(k) = \int_0^{\pi/2}(1-k^2\sin^2 t)^{-1/2}\,dt \tag{36}$$

$$E(k) = \int_0^{\pi/2}(1-k^2\sin^2 t)^{1/2}\,dt \tag{37}$$

Values of $K(k)$ and $E(k)$ may be obtained from standard tables or from readily available computer software.

$L_3(\beta)$ may likewise be reduced to an expression involving $K(k)$ and $E(k)$. However, for most practical cases, the factor $(\delta/r_0)^2$ by which $I_3(\beta)$ is multiplied is so small that the contribution to ΔR from the term proportional to $I_3(\beta)$ is negligible.

3. RESULTS

To illustrate the changes in impedance as a function of the liftoff distance l and the conductivity σ, calculations were made for a loop of radius $r_0 = 1.27$ cm (diameter of 1 in.) at distances l from 0.05 to 1.5 cm, and for conductivities from 0.1 to 4 times that of aluminum ($\sigma_0 = 3.8\times10^7$ mho/m). These results are shown in Figs. 2 and 3 as a function of l for various constant conductivities. The normalized dimensionless changes in impedance $\Delta X/\omega\mu r_0$ and $\Delta R/\omega\mu r_0$ are chosen as the quantities to be plotted. For all values of conductivity, the value of $\Delta X/\omega\mu r_0$ is seen

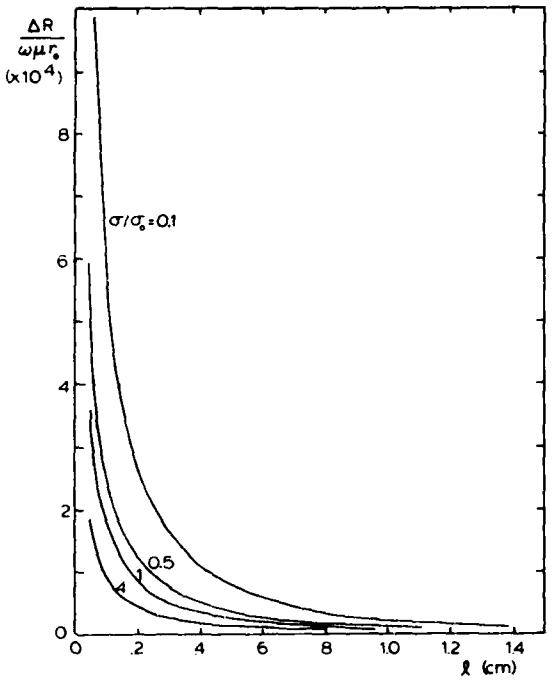

Fig. 2. Change in normalized resistance versus liftoff distance.

to approach a large negative value as l decreases, showing the known decrease in total inductance as the loop approaches the plane. As l becomes large, $\Delta X/\omega\mu r_0$ approaches zero as required. Similarly, in Fig. 2 $\Delta R/\omega\mu r_0$ is seen to give a large positive contribution for small l, and approaches zero as l becomes large.

To illustrate the effects of the conductivity on the changes in impedance for several constant values of liftoff, the results for the same loop are shown in Figs. 4 and 5. The change in reactance $\Delta X/\omega\mu r_0$ is seen to be very nearly independent of conductivity over the range considered. The value of $\Delta R/\omega\mu r_0$, however, is seen to increase for lower values of σ. This resistance term, of course, approaches zero as the conductivity approaches that of a perfect conductor.

Both the variations in resistance and reactance can be combined into the one graph shown in Fig. 6 by plotting ΔX versus ΔR. The solid lines thus show the change in impedance as the liftoff is changed, while the dashed lines show the variation with changing conductivity for constant liftoff l. Figure 6 represents a narrow strip of a conventional normalized impedance plane showing curves of constant conductivity and curves of constant liftoff, the strip corresponding to large values of conductivity, with the scale of normalized resistance greatly amplified in relation to the scale of normalized reactance. In a complete impedance plane representation, the curves of constant conductivity and curves of constant liftoff would, of course, converge at the origin.

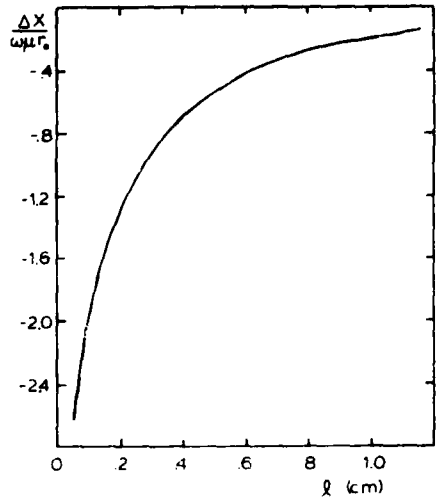

Fig. 3. Change in normalized reactance versus liftoff distance.

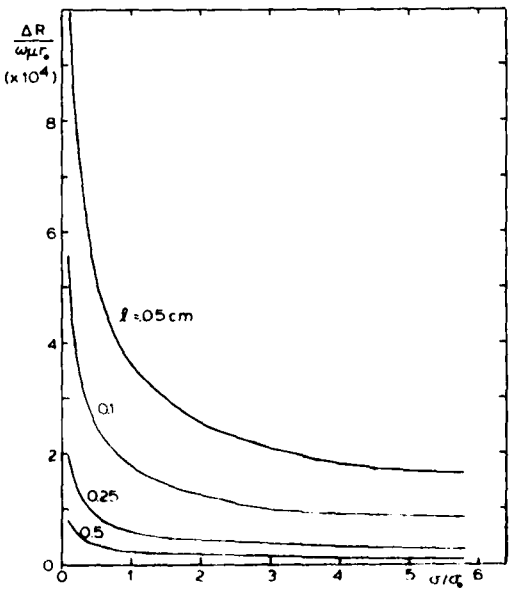

Fig. 4. Change in normalized resistance versus conductivity.

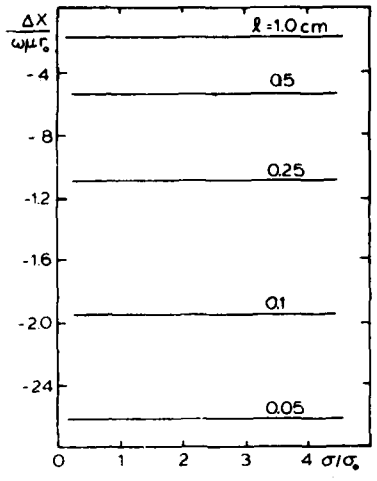

Fig. 5. Change in normalized reactance versus conductivity.

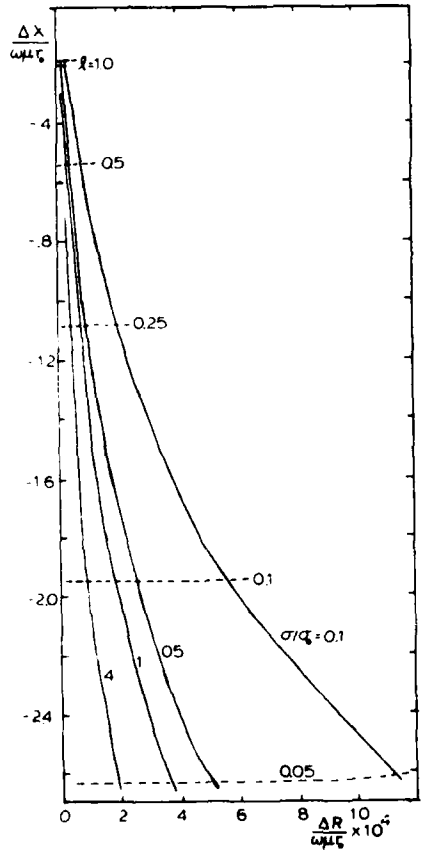

Fig. 6. Change in reactance versus change in resistance.

Table I. Comparison of Theoretical Change in Inductance to Mutual Inductance for the Perfect Conductor Case

l (cm)	$\frac{\Delta X}{\omega\mu r_0}$	ΔL (μH)	M (μH)
2.5	1.0887	0.01737	0.01727
5.0	0.5425	0.00866	0.00869
15.0	0.07784	0.00124	0.00114

The limiting values of $\Delta X/\omega\mu r_0$ for large values of σ can be checked by comparing the calculated values with that of the case of a loop above a perfectly conducting plane. Using image theory, the mutual inductance between two identical loops located a distance $2l$ apart can be calculated[6]:

$$M = 2.54 N r_0$$

where N is a tabulated function of r_0 and l. The values of M and ΔL at 50 KHz are compared in Table I, and quite good agreement is found.

4. CONCLUSIONS

For the commonly occurring case where $\delta \ll 0.1\ r_0$, the change in coil inductance is essentially the value that would occur if the substrate were perfectly conductive; ΔL is thus dominated by its dependence on liftoff. The change in resistance is, for constant liftoff, proportional in first order to skin depth (or, for constant frequency, proportional to the square root of substrate conductivity); however, ΔR is also strongly dependent upon liftoff. Second-order changes in ΔL and ΔR, due to small variations in l and σ about nominal values, are well approximated by linear functions of Δl and $\Delta\sigma$; hence variations in ΔL and ΔR may readily be interpreted in terms of corresponding variations in liftoff and conductivity.

ACKNOWLEDGMENTS

This work was supported in part by the U.S. Air Force Office of Scientific Research through Grant No. 77-3457.

REFERENCES

1. David H. S. Cheng, The reflected impedance of a circular coil in the proximity of a semi-infinite medium, *IEEE Trans. Instrumentation and Measurement*, 14 (3): 107–116 (September 1965).

2. C. V. Dodd and W. E. Deeds, Analytical solutions to eddy-current probe-coil problems, *J. Appl. Phys.* 39 (6): 2829–2838 (1968).
3. G. Arfken, *Mathematical Methods for Physicists*, 2nd ed. (Academic, New York, 1970), p. 495.
4. A. Erdelyi et al., *Tables of Integral Transforms* (McGraw-Hill, New York, 1954), Vol. 1, p. 183.
5. M. Abramowitz and I. Stegun, *Handbook of Mathematical Functions*, 9th ed. (Dover Publications, New York, 1970), pp. 334–337.
6. F. E. Terman, *Radio Engineers Handbook*, (McGraw-Hill, New York, 1943), p. 67.

APPENDIX C

Nondesctructive Evaluation of Dielectric Layers on Conductive Substrates by Microwave Surface Electromagnetic Waves

NONDESTRUCTIVE EVALUATION OF DIELECTRIC LAYERS ON CONDUCTIVE SUBSTRATES BY MICROWAVE SURFACE ELECTROMAGNETIC WAVES

C. G. Gardner, S. A. Long, and W. Ou

Electrical Engineering Department
University of Houston
Houston, Texas 77004

Abstract

The thickness and permittivity (or dielectric constant) of dielectric layers on electrically conductive substrates can be determined by suitable measurements using surface electromagnetic waves. The approach used here is to measure the cutoff frequency of the TM_1 SEW mode and, in effect, the propagation constant of the TM_1 SEW mode as a function of frequency. The theory of the method and some preliminary results obtained using 8-12GHz SEW supported by a layer of polypropylene on an aluminum substrate are presented. By going to higher frequencies the method can be extended to thin protective coatings on metals, e.g., ceramic coatings on jet engine and coal utilization components.

INTRODUCTION

The idea of using surface electromagnetic waves (SEW) to measure the thickness and dielectric constant (or complex permittivity) of a layer of dielectric material on an electrically conductive substrate is well known. It has received considerable attention in relation to opto-electronic devices in which thin layers of optically transparent material on conductive or semiconductive substrates are used as optical waveguides.[1,2] The possibility of adapting the technique for nondestructive evaluation of other types of coatings was raised by Bell and coworkers.[3] However, the idea does not appear to have been pursued to the point of practical application.

There are currently several potential applications of the method. Several in particular are noteworthy. One is the case of protective coatings on components of jet engines, coal combustion chambers, magnetohydrodynamic generators, and the like.[4] Another is the case of polymeric coatings for environmental protection. There is also the case of surfaces of metals prepared for adhesive bonding, where the strength attained by the bond is known to be sensitive to the condition of the adherent surfaces.

This paper describes some preliminary work exploring some of the possibilities and practical problems associated with the SEW method. It is not aimed at a specific application. The work involves the use of microwaves in the 8-12 GHz range (free space wavelengths around 3 cm). "Coatings" are simulated by relatively thick (~1.5 cm) slabs of a readily available plastic (polypropylene) placed on a large sheet of aluminum. For application to thin coatings, the techniques would have to be "scaled down" by one or two orders of magnitude. Fortunately there are no fundamental obstacles to this. Thus far only transverse magnetic (TM) waves have been used; the possibility of using transverse electric (TE) waves and combined TM and TE waves remains open.

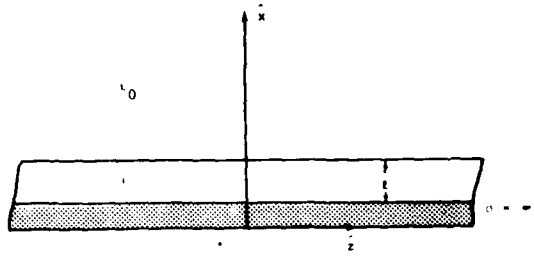

Figure 1. Dielectric Layer on Metal Substrate

THEORY

Referring to Figure 1, the illustrated unbounded planar structure can be shown from Maxwell's equations to support TM plane waves propagating in the z-direction (with surfaces of constant phase perpendicular to the z-direction) for which the z-component of the amplitude of the electric field is given by the relations:

$$E_z(x) = \begin{cases} E_0 \sin \kappa x & 0 \le x \le \ell \\ E_0 (\sin \kappa \ell) e^{-\kappa_0 (x-\ell)} & \ell < x \end{cases} \qquad (1)$$

where

$$\kappa_0 = (\beta^2 - k_0^2)^{1/2} \qquad (2)$$

$$\kappa = (\varepsilon k_0^2 - \beta^2)^{1/2} \qquad (3)$$

β is the propagation constant, and $k_0^2 = \omega^2 \mu_0 \varepsilon_0$. ε is the permittivity of the dielectric layer of thickness ℓ. Conditions for such a surface wave exist when the relation

$$k_0 \le \beta \le \varepsilon^{1/2} k_0 \qquad (4)$$

is satisfied. For this case, both κ and κ_0 are real, positive quantities.

The remaining components of the electric field intensity, as well as the y-component of the magnetic field intensity follow from Maxwell's equations (the x-component and z-component vanish). When the requisite boundary conditions on the fields are imposed, the following dispersion relation is found:

$$(\kappa \ell) \tan(\kappa \ell) = \varepsilon \kappa_0 \ell \qquad (5)$$

Equation (5) implicitly defines the propagation constant, β, as a function of k_0, ℓ and ε. This transcendental equation cannot be solved exactly in closed form. If Equation (5) is rewritten in the form

$$x \tan x = \varepsilon [(\varepsilon - 1)(k_0 \ell)^2 - x^2]^{1/2} \qquad (6)$$

where

$$x = \kappa \ell$$

it becomes clear that the solutions of the equation correspond to the intersection of the (circular) curve

$$y = \varepsilon [(\varepsilon - 1)(k_0 \ell)^2 - x^2]^{1/2}$$

with the curve

$$y = x \tan x .$$

Multiple solutions to the equation occur, a new branch occurring as x increases by a multiple of π. For $x = n\pi$, the right hand side of Equation (6) must vanish, ie.,

$$k_n = \frac{n\pi}{\ell(\varepsilon - 1)^{1/2}}, \quad n = 0, 1, \ldots \qquad (7)$$

The values of k_n given by Equation (7) correspond respectively to cutoff frequencies

$$\omega_n = \frac{n\pi c}{\ell(\varepsilon - 1)^{1/2}} \qquad (8)$$

where $c = (\mu_0 \varepsilon_0)^{-1/2}$ is the speed of light in vacuo. The fields corresponding to the solution of Equation (6) for $n\pi < x < (n+1)\pi$ are described as the TM_n SEW modes. The cutoff frequency for the TM_0 mode is, of course, zero; the TM_0 mode can be excited for any frequency. The higher order modes can be excited only for frequencies exceeding their respective cutoff frequencies. We note that a determination of the cutoff frequency of any mode except TM_0 determines the quantity $\ell(\varepsilon - 1)^{1/2}$.

If the left and right hand sides of Equation (6) are expanded as a power series in x about the

value $x = n\pi$, an approximate solution is obtained which may be written in the form

$$(\frac{\beta}{k_0})^2 = 1+((\frac{\varepsilon-1}{\varepsilon})\ell)^2(k_0-k_n)^2 \qquad (9)$$

Equation (9) is valid for

$$k_0 \gtrsim k_n .$$

Equation (9) may be written

$$[(\frac{\beta}{k_0})^2-1]^{1/2} = |(\frac{\varepsilon-1}{\varepsilon})\ell|(k_0-k_n) \qquad (10)$$

Thus if the propagation constant β is determined as a function of the wave number k_0 (for fixed values of ε and ℓ), for values of k_0 greater than, but near k_n, the quantity $(\varepsilon-1)\ell/\varepsilon$ may be determined as the slope of a graph of $[(\beta/k_0)^2 -1]^{1/2}$ versus k_0; the graph will intersect the k_0-axis at the value k_n, which, in turn, determines the quantity $\ell(\varepsilon-1)^{1/2}$. Writing

$$s = (\frac{\varepsilon-1}{\varepsilon})\ell \qquad (11)$$

we have

$$\varepsilon = \frac{1+[1-4(\frac{sk_n}{n\pi})^2]^{1/2}}{2(\frac{sk_n}{n\pi})^2} \qquad (12)$$

and

$$\ell = (\frac{\varepsilon}{\varepsilon-1})s \qquad (13)$$

Thus ε and ℓ are determined as functions of the experimentally measurable parameters s and k_n.

PRISM METHOD OF LAUNCHING AND RECEIVING SEW

One practical means of launching a SEW is Otto's prism method,[5] illustrated in Figure 2. If the angle of incidence ϕ is such that the internal angle of incidence θ exceeds the critical angle for the prism-air interface, then the x-component of the (now complex) propagation vector for the field below the prism is pure imaginary. By varying the angle of incidence ϕ (and consequently the internal angle of incidence θ), the ratio β/k_0 can (for appropriate of k_0) be made to assume the value

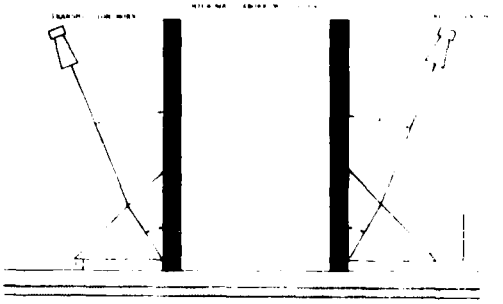

Figure 2. Prism Coupling Arrangement for Launching and Receiving Surface Electromagnetic Waves

necessary for a SEW on the substrate. At this condition, a SEW will propagate. Thus the condition for launching a TM_n surface wave may be written

$$\varepsilon_p^{1/2}\sin\theta = \frac{\beta}{k_0} = [1+(\frac{\varepsilon-1}{\varepsilon}\ell)^2(k_0-k_n)^2]^{1/2} \qquad (14)$$

where ε_p is the relative permittivity of the prism material.

If the wave inside the prism, and incident on the prism-air interface, were an ideal plane wave, there would be a sharply defined internal angle of incidence θ, at which a TM_n SEW could be launched. In practice the incident wave comprises plane waves with a range of propagation directions distributed about a central ray. Hence as θ is varied, the amplitude of the launched TM_n wave varies and is maximum for the theoretical value of θ. By measuring the value of θ at which the amplitude of the TM_n SEW is maximum, as a function of k_0 (or, equivalently, the frequency of the incident radiation), β/k_0 is determined as a function of k_0, and Equations (10), (12) and (13) may be applied to determine ε and ℓ.

EXPERIMENTAL METHOD

A block diagram of the experimental arrangement

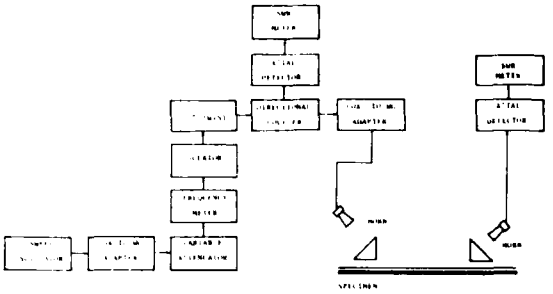

Figure 3. Block Diagram of Experimental Arrangement

is shown in Figure 3. A sweep oscillator which has a frequency range from 8.0 GHz to 12.4 GHz is used as the microwave source. For launching a surface electromagnetic wave, the prism coupling technique has been used. The 45° prisms were made of paraffin wax having a measured permittivity $\epsilon_p = 2.22$; the base size of the prisms is 20 cm × 20 cm. In order to minimize direct pick-up of any radiation other than SEW modes, two microwave absorbing screens were placed behind (or ahead of) the prisms. A gap of 9 cm was left between the microwave absorber and the specimen on which SEW propagated. Each microwave horn has an aperture 8 cm × 8 cm. In order to get a far-field pattern we have to set the distance between the transmission horn and prism $r > 2D^2/\lambda$, where D is the dimension of the aperture. For our case, r has to be greater than 45 cm. A divided circular quadrant (not shown in the figure) with a radius of 80 cm was built and the transmission horn mounted on it. For the receiving horn a similar scanning device with smaller radius (r = 50 cm) is used. The transmission and receiving horns can be independently scanned through 90°.

For coupling the wave in the prism into the SEW, there must be an air gap between the prism and the dielectric layer. Experiment shows the optimum gap for the best-coupling is $h = \lambda/2$, where λ is the free-space wavelength of the microwaves.

An aluminum sheet (alloy #6061) of size 8"×8" is used as the conductive substrate. Several polypropylene sheets of the same size but different thicknesses are used as the dielectric coating material. The polypropylene sheets are layed on the aluminum sheet and clamped in order to minimize air space between the polypropylene and the aluminimum sheet.

There are two basic parameters we have to measure, namely the frequency and the incident angle in the air. Before making quantitative measurements we have to scan several times to determine the angular range within which the TM_0 and TM_1 modes propagate with maximum amplitude.

In the actual measurement, as the external angle ϕ is increased, we have to adjust the position of the prism slightly in order to keep the central ray of the incident beam near the edge of the prism for most efficient coupling. Then the coupling angle can be obtained by scanning the incident beam from $\phi = 0°$ to $\phi = 80°$ and measuring the angle at which the most energy is coupled into the surface mode. The microwave frequency is obtained from the frequency meter.

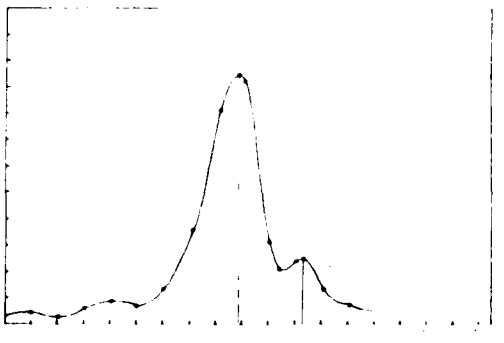

Figure 4. Surface Wave Intensity Versus External Angle of Incidence

RESULTS

Figure 4 is a representative graph of the detected signal amplitude as a function of the external angle of incidence. The large peak corresponds to the TM_1 mode; the smaller second peak corresponds to the TM_0 mode. Table 1 shows an example of measurements obtained from a specimen of thickness ℓ = 1.50 cm and the dielectric constant of the polypropylene layer ϵ = 2.25. There are two modes (TM_1 and TM_0) which can be propagated on this structure. The data in Table 1 is the result of the TM_1 mode, because only the higher mode is useful to determine the dielectric constant and thickness of the layer. The table basically contains the frequency f and the incident angle in the air, ϕ; the other data is simply determined from f and ϕ. The free-space wave number is $k_0 = 2\pi f/c$, where c is the velocity of light in free space. The incident angle in the prism, θ, is obtained from the incident angle in the air, ϕ. There are two cases: i) For $\phi < \pi/4$ then $\theta = \pi/4 - \sin^{-1}(\sin(\pi/4-\phi)/n_p)$; ii) If $\phi > \pi/4$ then $\theta = \pi/4+\sin^{-1}(\sin(\phi-\pi/4)/n_p)$, where n_p is the refraction index of the prisms ($n_p = \sqrt{\epsilon_p}$). The most important parameter we must know is the ratio β/k_0. According to the theory of launching SEW by the prism coupling technique, the incident angle in the prism is determined by the equation $\beta = k_0 n_p \sin\theta$; therefore if we know θ and n_p, β/k_0 can be obtained from the equation $\beta/k_0 = n_p \sin\theta$. β/k_0 in turn determines the quantity $[(\beta/k_0)^2-1]^{1/2}$.

The approximate dispersion relation for any TM_n mode of SEW near cutoff is given by Equation (9). From Equation (10) we can see that if we plot $[(\beta/k_0)^2-1]^{1/2}$ versus k_0, a straight line will result, and the slope s will be equal to $(\epsilon-1)/\epsilon\ell$; the intercept will be equal to the cutoff wave number k_1. A representative graph corresponding to the data in Table 1 is shown in Figure 5. For this particular case, the slope $s = 8.39 \times 10^{-3}$ m and $k_1 = 186.7\ m^{-1}$. After s and k_1 are determined, ϵ and ℓ are obtained by means of Equations (12) and (13). For the example, we have ϵ = 2.16 and ℓ = 1.56 cm. These may be compared with the value ϵ = 2.25 determined by the standard waveguide method, and ℓ = 1.50 cm measured with a pair of calipers.

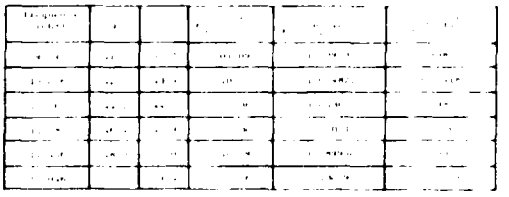

Table 1. Representative Data for TM_1 SEW on 1.5 Inch Polypropylene Layer on Aluminum Substrate

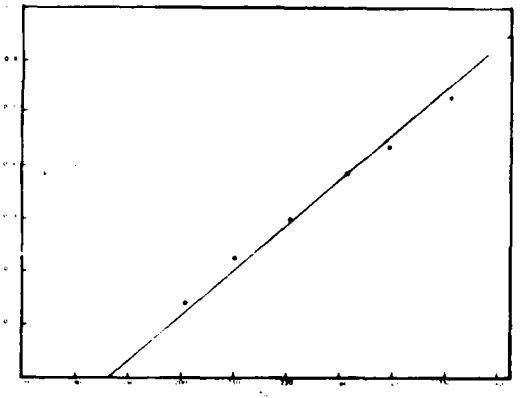

Figure 5. Function of Surface Wave Propagation Constant Versus Wave Number of Exciting Radiation

CONCLUSION

The possibility of measuring the thickness and dielectric constant of a dielectric layer on a conductive substrate by measuring the propagation constant of a TM SEW using the prism launching method has been demonstrated in a regime appropriate to the 8-12 GHZ frequency range. To handle thinner dielectric layers it

will be necessary to employ much higher frequencies.

A number of important points remain to be investigated, including: (1) the effects of pronounced variations in the thickness of the dielectric layer; (2) the effects of pronounced variations in the dielectric constant of the dielectric layer; and (3) the effects of imperfections in the surface of the conductive substrate.

In order to rationally optimize the experimental arrangement it will be necessary to develop a detailed mathematical model of the prism SEW launching arrangement.

Finally, it would be worthwhile to investigate alternative launching arrangements including gratings (or similar periodic structures) and special horns; and to investigate the possibilities of using transverse electric (TE) modes as well as both TM and TE modes.

ACKNOWLEDGEMENT

This work was supported in part by the U. S. Air Force Office of Scientific Research through Grant #77-3457.

REFERENCES

1. Ulrich, R., and Torge, R., Measurement of Thin Film Parameters with a Prism Coupler, Applied Optics, Vol. 12, No. 12, pp. 2901-2908 (1973).

2. Chung, P. S., Multi-Wavelength Determination of Single-Mode Optical Waveguide Parameters, Optica Acta, Vol. 23, No. 8, pp. 651-663 (1976).

3. Bell, R. J., and Alexander, R. W., Jr., The Use of Surface Electromagnetic Waves to Measure Materials Properties, J. Non-Crystalline Solids, Vol. 19, pp. 93-103 (1975).

4. Scott, G. W., et al., Nondestructive Inspection of Thin Plasma-Sprayed Ceramic and Cermet Protective Coatings for Coal Conversion and Utilization Equipment, ORNL/TM-6210, Oak Ridge National Laboratory, Oak Ridge, Tennessee, April, 1978, (Available from National Technical Information Service, Springfield, Va. 22161).

5. Otto, A., Excitation of Nonradiative Surface Plasma Waves in Silver, Z. Physik, Vol. 216, pp. 398-410 (1968).

APPENDIX D

The Change in Impedance of a Single-Turn Coil Due to a Void in a Conducting Half Space

THE CHANGE IN IMPEDANCE OF A SINGLE-TURN COIL DUE TO A VOID IN A CONDUCTING HALF SPACE

Afroz J. M. Zaman, C. Gerald Gardner, and Stuart A. Long
Department of Electrical Engineering
University of Houston
Houston, Texas 77004

Abstract

The problem of detection and characterization of a flaw in a conducting half-space using an eddy-current coil oriented parallel to the interface is examined. An expression is derived for a first order approximation for the change in complex impedance due to a void located within the conducting medium. The overall impedance is a function of the radius and lift-off distance of the test coil and the conductivity of the material. An analytical expression is derived for the change in impedance as a function of the electric fields at the position of the flaw. It is found to be an integral over the volume of the flaw of the electric fields found with and without the flaw being present. The limiting case of a degenerate point flaw may be examined in greater detail by allowing the field in the presence of the flaw to be approximated by the unperturbed field. For flaws small enough that the field does not vary much over its volume the field may be even further approximated by using just the value of the field at the position of the centroid of the flaw. Plots are shown to illustrate the behavior of the change in impedance as a function of the radial range of the flaw and the depth of the flaw centroid, using previously derived expressions for the fields for the unflawed case.

1. INTRODUCTION

In previous work, an approximate analytical expression for the change in impedance of a single turn loop parallel to and near a conducting half space has been obtained analytically for certain idealized test coil and specimen configurations.[1] The results of this previous investigation have been used to calculate the change in impedance due to a finite flaw in the conducting material. An analytical expression has been derived for a first order approximation for the change in the complex impedance due to a small void within the conducting medium as a function of the electric field at the position of the flaw. A knowledge of the fields everywhere in the conducting medium due to the impressed source current of the loop is required. The change in coil impedance ΔZ due to the void can be found in terms of an integral of the field quantities $\vec{E}$ and $\vec{E}_0$ (the fields at the position of the flaw with and without the flaw being present). The electric field inside the conducting material can be obtained from the standard boundary value problem approach in terms of an integral

over a separation parameter. A series expansion of the integrand then allows the field to be expressed in terms of a derivative of the Legendre function of the second kind of half order. The field expressions substituted in the equation for ΔZ give the complex impedance as a function of the depth and radial position of the flaw. The radial position affects only in the magnitude but changes in the depth result in variations in both the magnitude and phase. This can be explained by the fact that for our eddy current approximations the radial position of the loop will always be a negligibly small portion of the wavelength in air. However, the depth in the conducting material is not small compared to the skin depth and therefore affects the phase of the response.

2. BASIC THEORY

Consider a two port network consisting of a transmitter T; a receiver R and a conductive body B containing an internal void of volume V_F as shown in Fig. 1. Then identify the multiply connected region bounded by the surface S_F of the void; the closed surface S_T surrounding the transmitter and the associated guiding structure (a portion of which coincides with a standard reference plane cutting through the field guiding structure); a similar surface S_R for the receiver; and a boundary at infinity S_∞. Let the volume enclosed by this surface be V, and let $\vec{E}_0$ and $\vec{H}_0$ denote the time harmonic fields that would exist when the material within V_F is identical to that within V_B and $\vec{E}$ and $\vec{H}$ denote the field actually existing with the void present.

Since the volume V contains no sources and the material within V is identical with or without the presence of V_F, the Lorentz reciprocity theorem is valid. With the bounded volume V, $\vec{E}_0$, $\vec{H}_0$ and $\vec{E}$, $\vec{H}$ satisfy the same set of equations,

$$\nabla\times\vec{E} = -j\omega\mu_0\vec{H} \; ; \quad \nabla\times\vec{H} = j\omega\varepsilon(\vec{r})\vec{E}$$

By the Lorentz reciprocity theorem, we have

$$\int_S [\vec{E}_0\times\vec{H} - \vec{E}\times\vec{H}_0]\cdot d\vec{s} = 0$$

where $d\vec{s}$ is an element of surface which is normal to and directed into the bounded volume. The surface S is the sum of surfaces which include S_∞, S_T, S_R and S_F

But $$\int_S = \int_\infty + \int_{S_T} + \int_{S_R} + \int_{S_F} = 0$$

Since the tangential component of elec-

tric field intensity vanishes on the metal waveguide by the boundary condition, $\int_{\text{boundary surface}} = 0$; and since the fields satisfy the radiation condition, the integral over S_∞ vanishes. Hence, we have

$$\int_{S_T+S_R} [\vec{E}_0\times\vec{H}-\vec{E}\times\vec{H}_0]\cdot d\vec{s} = -\int_{S_F} [\vec{E}_0\times\vec{H} - \vec{E}\times\vec{H}_0]\cdot d\vec{s}$$

Given the assumption that the transmitter and receiver waveguides operate in their respective dominant modes, currents and voltages are defined such that

$$\vec{E} = V\vec{e};\ \vec{H} = I\vec{h};\ \vec{E}_0 = V_0\vec{e};\ \vec{H}_0 = I_0\vec{h}$$

where $\vec{e}$ and $\vec{h}$ are the normalized dominant waveguide modal electric and magnetic fields; that is $\int_{\text{cross section}} (\vec{e}\times\vec{h})\cdot d\vec{s} = 1$, we have

$$\int_{S_T} (\vec{E}_0\times\vec{H}-\vec{E}\times\vec{H}_0)\cdot d\vec{s} = I_{T_0}V_T - I_T V_{T_0}$$

$$\int_{S_R} (\vec{E}_0\times\vec{H}-\vec{E}\times\vec{H}_0)\cdot d\vec{s} = I_{R_0}V_R - I_R V_{R_0}$$

If $\vec{E}_0$, $\vec{H}_0$ are the fields with a current I_R impressed at the reference plane and the transmitter open circuited ($I_{T_0}=0$) and $\vec{E}$, $\vec{H}$ are the fields with an impressed current I_T and the receiver open-circuited ($I_R=0$), then

$$-I_T V_{T_0} + I_{R_0} V_R = -\int_{S_F} (\vec{E}_0\times\vec{H}-\vec{E}\times\vec{H}_0)\cdot d\vec{s} = 0$$

Now $V_{T_0} = Z_{12_0} I_{R_0}$, where Z_{12_0} is the transfer impedance between transmitter and receiver with no void; and $V_R = Z_{12} I_T$, where Z_{12} is the transfer impedance with the void.

Hence

$$I_{R_0} I_T (Z_{12}-Z_{12_0}) = -\int_{S_F} (\vec{E}_0\times\vec{H}-\vec{E}\times\vec{H}_0)\cdot d\vec{s}$$

$$\therefore\ \Delta Z_{12} \triangleq (Z_{12}-Z_{12_0}) = -\frac{1}{I_{R_0} I_T}\int_{S_F} (\vec{E}_0\times\vec{H}-\vec{E}\times\vec{H}_0)\cdot d\vec{s}$$

using Gauss' theorem

$$\Delta Z_{12} = -\frac{1}{I_{R_0} I_T}\int_{V_F} \nabla\cdot(\vec{E}_0\times\vec{H}-\vec{E}\times\vec{H}_0)\,dv$$

$$\Delta Z_{12} = -\frac{1}{I_{R_0} I_T}\int_{V_F} [\vec{H}\cdot(\nabla\times\vec{E}_0)-\vec{E}_0\cdot(\nabla\times\vec{H}) - \vec{H}_0\cdot(\nabla\times\vec{E})+\vec{E}\cdot(\nabla\times\vec{H}_0)]\,dv$$

$$= -\frac{1}{I_{R_0} I_T}\int_{V_F} [\vec{H}\cdot(-j\omega\mu_0\vec{H}_0)-\vec{E}_0\cdot(j\omega\varepsilon\vec{E}) - \vec{H}_0\cdot(-j\omega\mu_0\vec{H})+\vec{E}\cdot(j\omega\varepsilon_0\vec{E}_0)]\,dv$$

$$= \frac{j\omega(\varepsilon-\varepsilon_0)}{I_{R_0} I_T}\int_{V_F} \vec{E}_0\cdot\vec{E}\,dv$$

But $\varepsilon = \varepsilon_0 - \frac{j\sigma}{\omega}$ $\therefore$ $\varepsilon-\varepsilon_0 = -\frac{j\sigma}{\omega}$

$$\therefore\ \Delta Z_{12} = \frac{\sigma}{I_{R_0} I_T}\int_{V_F} \vec{E}_0\cdot\vec{E}\,dv$$

where $\vec{E}$ and $\vec{E}_0$ are respectively the electric fields found with and without the flaw being present. The limiting case of a degenerate point flaw may be examined in greater detail by allowing the field in the presence of the flaw ($\vec{E}$) to be approximated by the unperturbed field $\vec{E}_0$ over the volume of the flaw.

$$\Delta Z_{12} = \frac{\sigma}{I_{R_0} I_T}\int_{V_F} [E_0(r,z)]^2\,dv$$

For flaws small enough that the fields do not vary greatly over its volume, the expression may be further approximated by using just the value of the field at the position of the centroid of the flaw (r_c, z_c).

$$\Delta Z_{12} = \frac{\sigma V_F}{I_{R_0} I_T} [E_0(r_c, z_c)]^2$$

3. FLAW IN A HALF SPACE

The basic geometry of the problem is shown in Fig. 2 and consists of a single turn coil of radius "r_0" oriented parallel to and at a distance "ℓ" above a conducting half space within which a flaw of volume V_F is located at a position (r_c, z_c) with respect to the origin of the co-ordinate system.

The field in each region satisfies Maxwell's equation and hence the wave equation for the vector potential $\vec{A}$.

$$\nabla^2 \vec{A} + k^2 \vec{A} = -\mu \vec{J}_{impressed}$$

Making the usual quasistatic approximation in regions I and II (that the $k^2\vec{A}$ term is negligible) and with $k^2 = j\omega\mu\sigma$ in region III, the solution for $\vec{A}$ in the three regions is[1]

$$A_\phi^I(r,z) = \int_0^\infty B_1(\alpha) e^{-\alpha z} J_1(\alpha r) d\alpha$$

$$A_\phi^{II}(r,z) = \int_0^\infty [B_2(\alpha) e^{-\alpha z} + C_2(\alpha) e^{\alpha z}] \cdot J_1(\alpha r) d\alpha$$

$$A_\phi^{III}(r,z) = \int_0^\infty C_3(\alpha) e^{\alpha_1 z} J_1(\alpha r) d\alpha$$

Using the four boundary condition equations resulting from the continuity of $\vec{E}$ and $\vec{H}$ at $z = \ell$, and $z = 0$ the four constants can be found.

Our principal interest is evaluating the vector potential inside the conducting half space, which in turn gives the fields in that region. The simplest choice is to evaluate C_3 and use the expression for A_ϕ^{III} to calculate the time varying field.

The resulting derivation for the coefficient C_3 is

$$C_3 = \frac{\mu_0 i r_0 J_1(\alpha r_0) e^{-\alpha \ell}}{(1 + \frac{\alpha_1}{\alpha})}$$

where α is the separation variable and

$$\alpha_1 = \sqrt{\alpha^2 + j\omega\mu\sigma}$$

which gives

$$A_\phi^{III}(r,z) = \mu_0 i r_0 \int_0^\infty J_1(\alpha r) J_1(\alpha r_0) \cdot \frac{e^{-\alpha \ell} e^{\alpha_1 z}}{\alpha + \alpha_1} \alpha d\alpha$$

The effective range of the integration variable α for which the value of the integrand is significant is much smaller than the quantity $\omega\mu\sigma$. For such cases $\frac{\alpha}{\alpha+\alpha_1}$ may be expanded as a power series in $\frac{\alpha}{\sqrt{\omega\mu\sigma}}$

$$\frac{\alpha}{\alpha+\alpha_1} = \frac{\alpha}{\alpha_1 [1 + \frac{\alpha}{\alpha_1}]}$$

$$\frac{\alpha}{\alpha_1} = \frac{\alpha}{\sqrt{\alpha^2+j\omega\mu\sigma}} = \frac{1}{\sqrt{1+\frac{j\omega\mu\sigma}{\alpha^2}}}$$

For a good conductor $\omega\mu\sigma >> \alpha^2$ $\therefore$ $|\frac{\alpha}{\alpha_1}| << |$

$$\frac{\alpha}{\alpha+\alpha_1} = \frac{\alpha}{\alpha_1}\left[1-\left(\frac{\alpha}{\alpha_1}\right)+\left(\frac{\alpha}{\alpha_1}\right)^2-\left(\frac{\alpha}{\alpha_1}\right)^3+\ldots\ldots\right]$$

$$\alpha_1 \triangleq \sqrt{j\omega\mu\sigma} = (1+j)\frac{1}{\delta}$$

where $\delta = \sqrt{2/\omega\mu\sigma}$

$$\frac{\alpha}{\alpha_1} = \frac{1-j}{2}(\delta\alpha)$$

$$\left(\frac{\alpha}{\alpha_1}\right)^2 = -\frac{j}{2}(\delta\alpha)^2$$

$$\left(\frac{\alpha}{\alpha_1}\right)^3 = -\frac{(1+j)}{4}(\delta\alpha)^3$$

The vector potential in the conducting material as a power series in skin depth is

$$A_\phi^{III}(r,z) = \mu_0 i r_0 [\delta \int_0^\infty \frac{(1-j)}{2} J_1(\alpha r) \cdot J_1(\alpha r_0) e^{-\alpha\ell} e^{\alpha_1 z} \alpha d\alpha + \delta^2 \int_0^\infty \frac{j}{2} J_1(\alpha r) J_1(\alpha r_0) e^{-\alpha\ell} \cdot e^{\alpha_1 z} \alpha^2 d\alpha - \delta^3 \int_0^\infty \frac{(1+j)}{4} J_1(\alpha r) J_1(\alpha r_0) \cdot e^{-\alpha\ell} e^{\alpha_1 z} \alpha^3 d\alpha \ldots\ldots]$$

Using the Lorentz condition, $\vec{\nabla}\cdot\vec{A} = -\mu\varepsilon \frac{\partial\phi}{\partial t}$, for the present case with circular symmetry, $\vec{\nabla}\cdot\vec{A} = 0$, and the scalar potential ϕ must be time independent. This means ϕ will give rise only to a static field which is of little interest. Therefore,

$$\vec{E} \simeq -\frac{\partial\vec{A}}{\partial t} = -j\omega\vec{A}_\phi$$

So $\vec{E}_0$, the field without the presence of the flaw in the conducting half space is given by

$$\vec{E}_0 = \frac{\mu_0 i r_0}{2} \omega e^{(1+j)z/\delta}[j\int_0^\infty (1-j)\delta \cdot J_1(\alpha r) J_1(\alpha r_0) e^{-\alpha\ell} \alpha d\alpha - \int_0^\infty \delta^2 J_1(\alpha r) J_1(\alpha r_0) e^{-\alpha\ell} \alpha^2 d\alpha \ldots\ldots]$$

$$= \frac{\mu_0 i r_0}{2} \omega e^{(1+j)z/\delta}[j\int_0^\infty \delta J_1(\alpha r) \cdot J_1(\alpha r_0) e^{-\alpha\ell}\alpha d\alpha + \int_0^\infty \delta J_1(\alpha r) J_1(\alpha r_0) \cdot e^{-\alpha\ell}\alpha d\alpha - \int_0^\infty \delta^2 J_1(\alpha r) J_1(\alpha r_0) e^{-\alpha\ell} \cdot \alpha^2 d\alpha \ldots\ldots]$$

This series of terms may be expressed in the form of a Legendre function by taking the derivative of the Laplace transform of the quantity $J_1(\alpha r)J_1(\alpha r_0)$ [2]

$$\int_0^\infty J_1(\alpha r) J_1(\alpha r_0) e^{-\alpha\ell} d\alpha = \frac{1}{\pi\sqrt{r r_0}} \cdot Q_{1/2}\left(\frac{\ell^2+r^2+r_0^2}{2 r r_0}\right)$$

$$\int_0^\infty J_1(\alpha r) J_1(\alpha r_0) e^{-\alpha\ell} \alpha d\alpha = -\frac{d}{d\ell}\left[\int_0^\infty \cdot J_1(\alpha r) J_1(\alpha r_0) e^{-\alpha\ell} d\alpha\right] = I(\alpha)$$

$$\therefore I(\alpha) = -\frac{1}{\pi\sqrt{r r_0}} \frac{d}{d\ell} Q_{1/2}(x)$$

where $x = \frac{\ell^2+r^2+r_0^2}{2 r r_0}$

$$I(\alpha) = -\frac{\ell}{\pi (r r_0)^{3/2}} Q'_{1/2}(x)$$

From the recursion relation for Legendre functions, the derivative may be expressed in terms of the functions themselves. [3]

$$Q'_{1/2}(x) = \frac{1}{(x^2-1)}\left[\frac{x}{2}Q_{1/2}(x) - \frac{1}{2}Q_{-1/2}(x)\right]$$

Thus

$$\int_0^\infty J_1(\alpha r)J_1(\alpha r_0)e^{-\alpha\ell}\alpha d\alpha = -\frac{\ell}{\pi(rr_0)^{3/2}(x^2-1)} \cdot \left[\frac{x}{2}Q_{1/2}(x) - \frac{1}{2}Q_{-1/2}(x)\right]$$

$$= I(\alpha)$$

Neglecting terms of order δ^2 and above,

$$\vec{E}_0 = \frac{\mu_0 i r_0}{2}\omega e^{(1+j)z/\delta}[1+j]\delta I(\alpha)$$

For a small flaw located at $(r_c,-z_c)$ as shown in Fig. 2, $\vec{E}_0$ can be approximated as

$$\vec{E}_0 = \frac{\mu_0 i r_0}{2}\omega e^{-(1+j)z_c/\delta}[1+j]\delta I(\alpha)$$

Since the same coil is used as the primary coil and also as the secondary coil $I_T = I_R$ and

$$\Delta Z = \frac{\sigma V_F}{I_2}\vec{E}_0(\vec{r}_c)\vec{E}_0(\vec{r}_c)$$

$$\Delta Z = V_F\omega\mu_0 r_0^2[I(\alpha)]^2 e^{-2z_c/\delta}e^{-j2(z_c/\delta-\pi/4)}$$

From the expression for ΔZ above it is evident that all the dependence on radial position is contained in the $I(\alpha)$ term which contributes only to the magnitude of the change in impedance. The depth of the flaw is seen to affect both the magnitude and phase of the change in impedance.

The constant phase factor $e^{j\pi/2}$ comes from the first two terms of the series expansion of $\vec{A}_\phi$. This factor would shift slightly if more terms were included in the series expansion.

4. RESULTS

To illustrate the change in impedance as a function of the radial location of the flaw, the function $[I(\alpha)]^2 r_0^2$ is plotted versus r_c in Fig. 3 for several different liftoff distances varying from 0.3 to 1 times the radius of the loop. Each of these curves tends to zero as the flaw approaches the point directly under the center of the loop or as the distance from the periphery of the loop becomes large. Each curve attains its maximum value when the flaw is directly under the wire of the loop and the value of this maxima is a function of the liftoff distance. This behavior is to be expected since the induced eddy current distribution under the loop is zero at the center and a maximum at the position of the current carrying coil. The current density then decays as the position of the flaw moves further away from the loop. At any constant radial position, the magnitude of the eddy current density becomes larger as the liftoff becomes smaller. This functional dependence is shown in Fig. 4 for the case of $r_c = r_0$.

Since the axial position of the flaw affects both the magnitude and phase of the change in impedance, the real and imaginary parts of this factor have been plotted versus flaw depth in Fig. 5. As the flaw becomes more deeply imbedded inside the material the phase can change enough so that the reactive part of the impedance becomes negative near $z_c/\delta = \pi/4$. Similarly the resistive part passes through zero at $z_c/\delta = \pi/2$, but the magnitude has decayed to an almost negligible value for flaws at this depth.

The real part of the impedance is zero for a flaw at the surface (z_c=0) owing to the assumption that V_F is infinitesimally small. Thus when V_F is located at the surface, the current distribution is not affected.

For constant values of lift-off and depth

of the flaw the magnitude of the change in impedance is shown in Fig. 6 for linear scans of the coil near the flaw. Curves are shown for the coil moving parallel to the y-axis at x=0, x=0.5r_0, x=r_0, and x=1.5r_0 (see Fig. 2). The behavior is as expected with peaks at the points where the flaw is nearest the current carrying wire.

ACKNOWLEDGEMENT

This work was supported in part by the U. S. Air Force Office of Scientific Research through Grant 77-3457 and in part by the Energy Laboratory of the University of Houston.

REFERENCE

(1) A. J. M. Zaman, S. A. Long and C. G. Gardner, "The Impedance of a Single-Turn Coil Near a Conducting Space", Journal of Nondestructive Evaluation, Vol. 1, No. 3, Sept. 1980, pp. 183-189.

(2) A. Erdelyi et al., Tables of Integral Transforms, McGraw-Hill, New York, 1954, Vol. 1, p. 183.

(3) M. Abramowitz and I. Stegun, Handbook of Mathematical Functions, 9th ed, Dover Publications, New York, 1970, pp. 334-337.

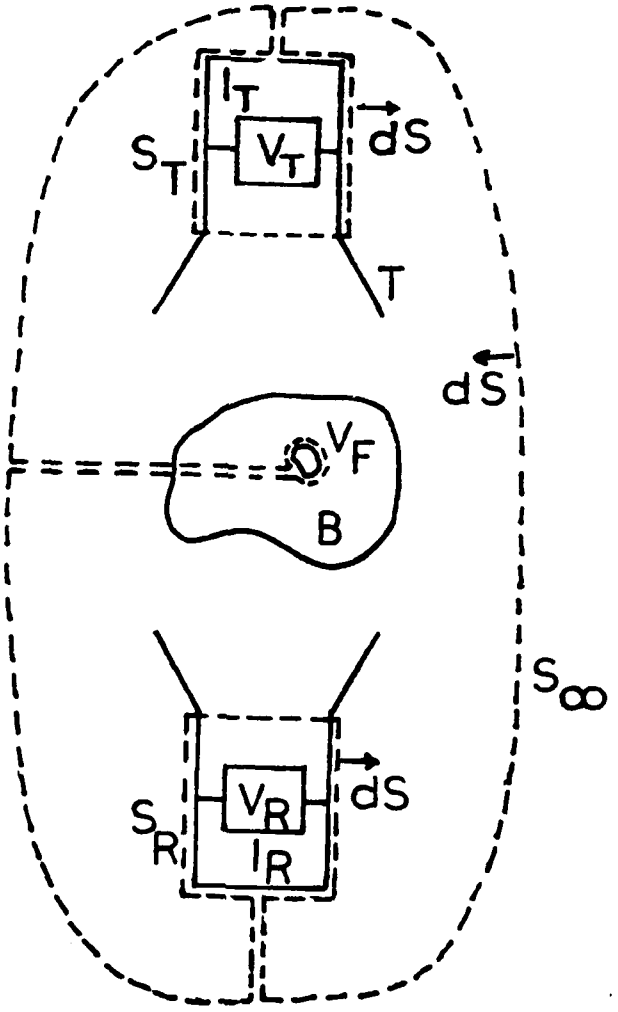

Fig. 1 Generalized problem

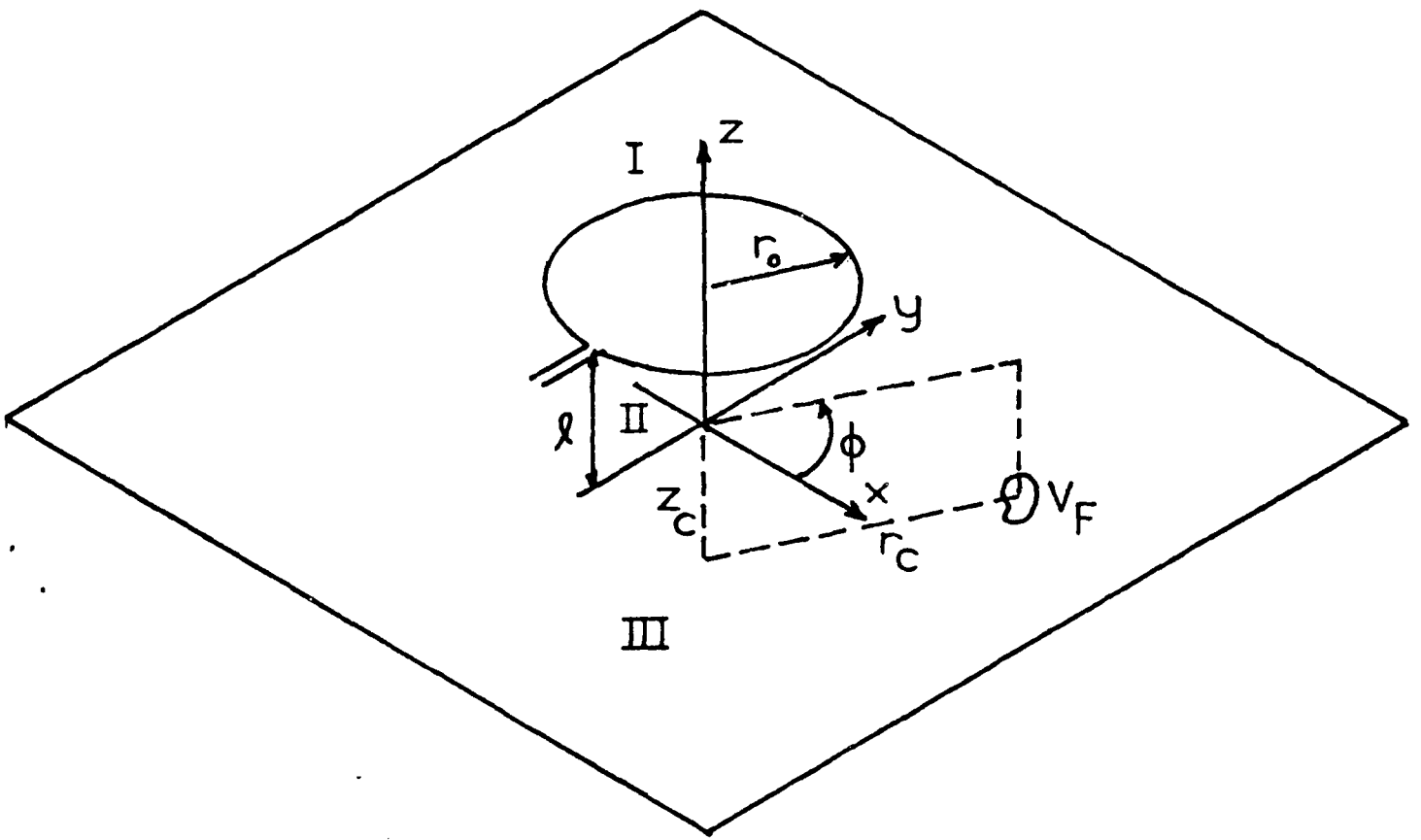

Fig.2 Loop near a conducting half space

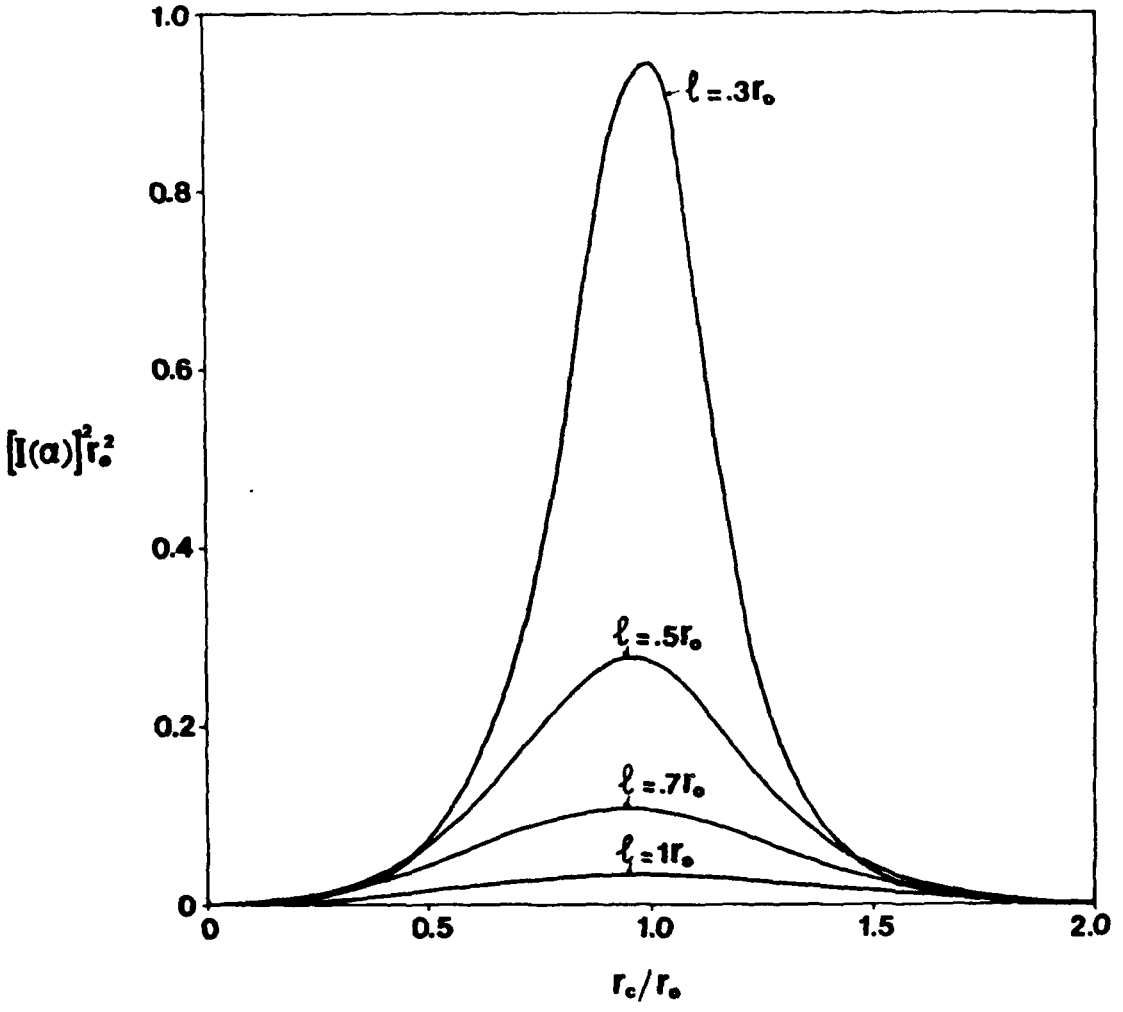

Figure 3. Magnitude of eddy current response versus radial position of flaw.

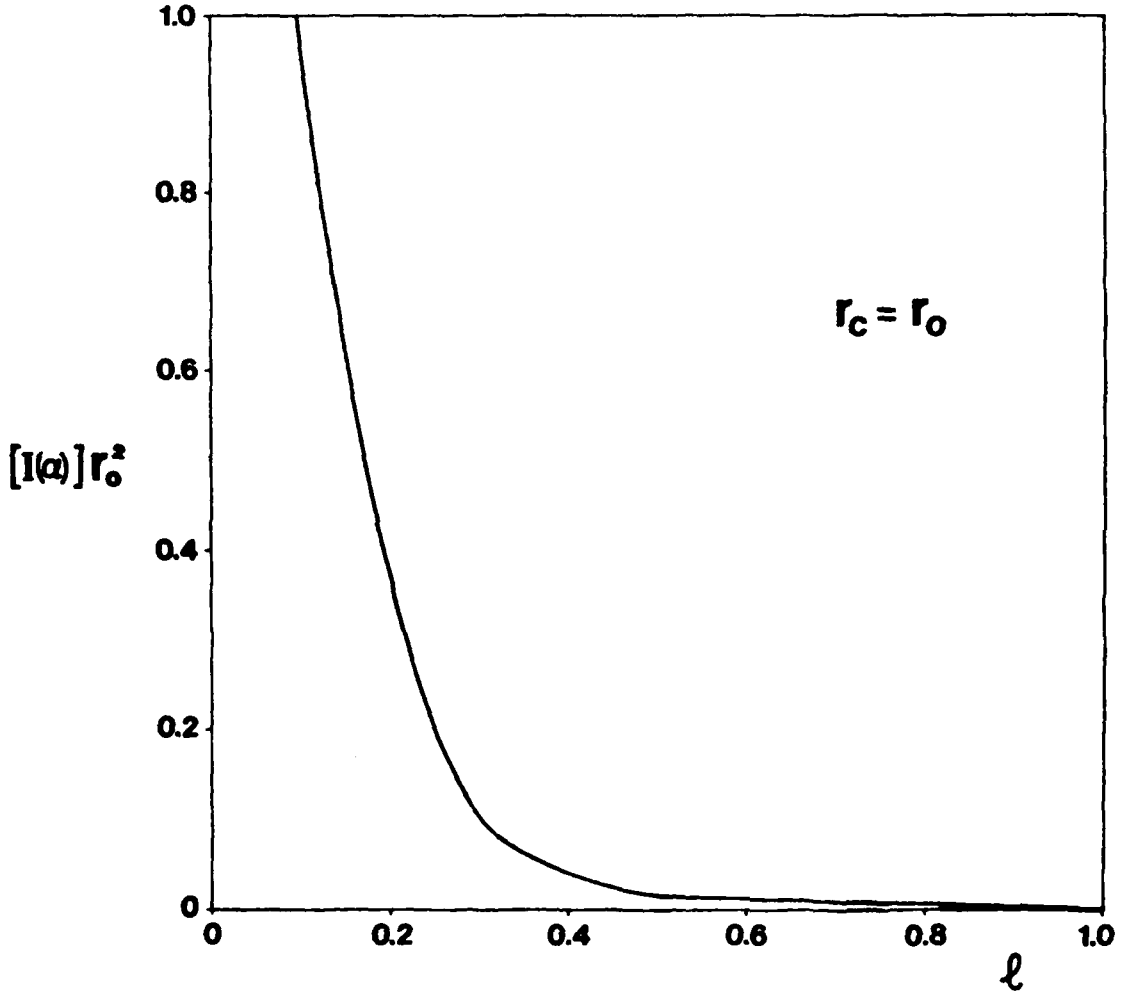

Figure 4. Magnitude of eddy current response versus lift-off distance.

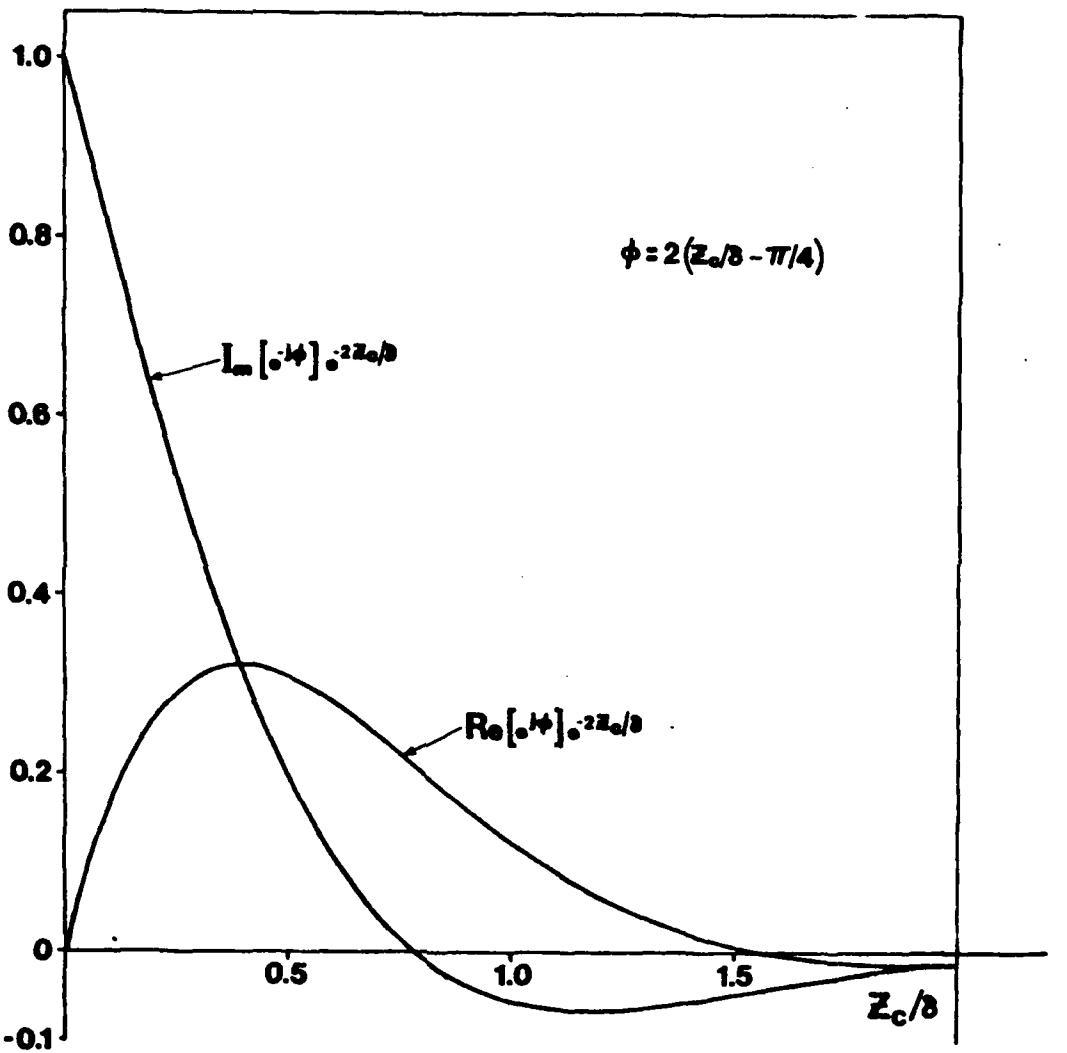

Figure 5. Real and imaginary parts of eddy current response versus depth of flaw.

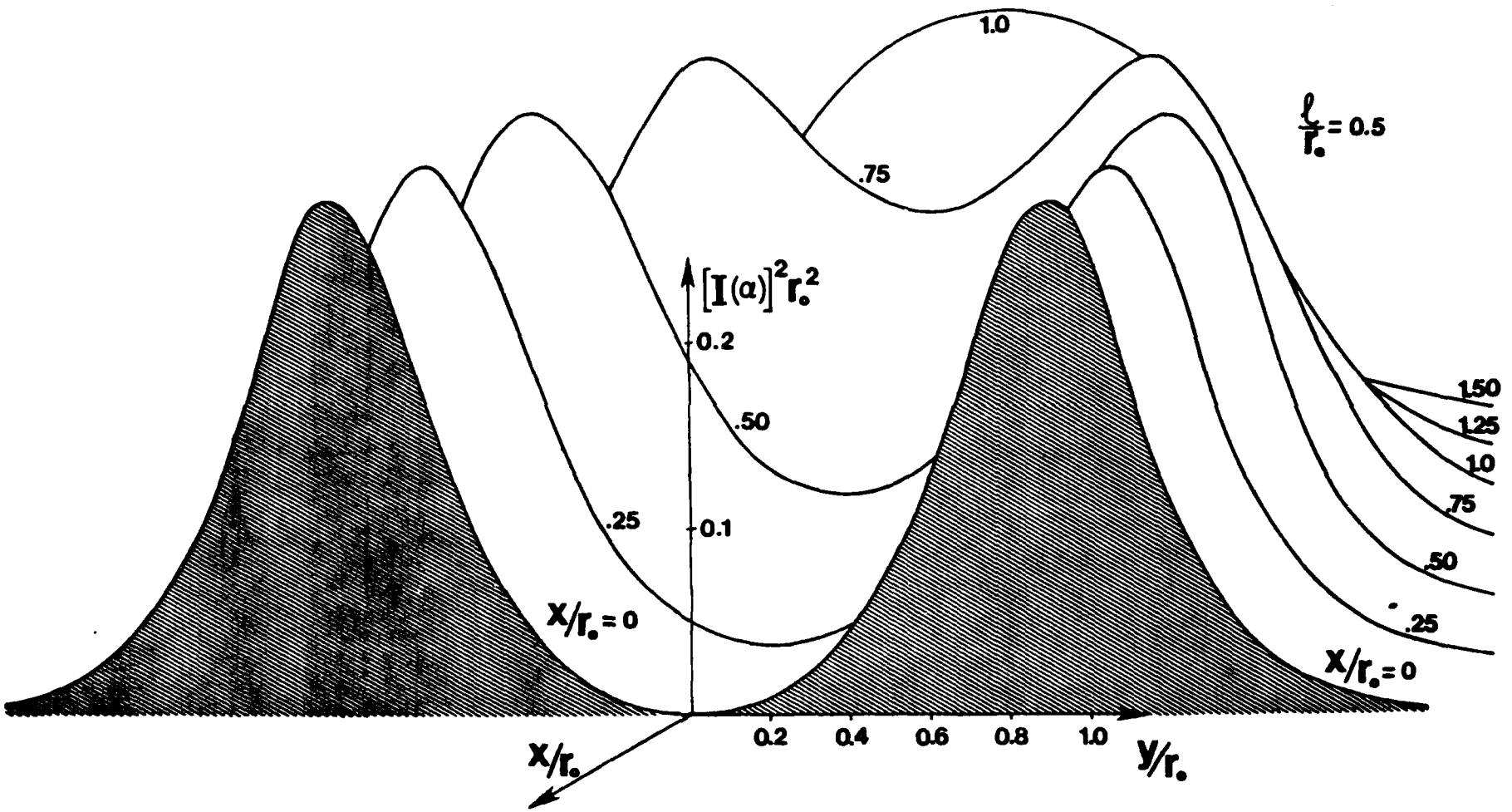

Figure 6. Magnitude of eddy current response versus scan position.


FILME
8